SERI/STR-211-2923
DE86004449

April 1986

$CuInSe_2$ Solar Cell Research by Sputter Deposition

Annual Subcontract Report
1 December 1984 - 31 December 1985

J. A. Thornton
T. C. Lommasson
A. F. Burnett
University of Illinois
Urbana, Illinois

Prepared under Subcontract No. XL-5-04131-1

SERI

Solar Energy Research Institute
A Division of Midwest Research Institute

1617 Cole Boulevard
Golden, Colorado 80401-3393

Operated for the
U.S. Department of Energy
under Contract No. DE-AC02-83CH10093

Printed in the United States of America
Available from:
National Technical Information Service
U.S. Department of Commerce
5285 Port Royal Road
Springfield, VA 22161

Price: Microfiche A01
Printed Copy A05

Codes are used for pricing all publications. The code is determined by the number of pages in the publication. Information pertaining to the pricing codes can be found in the current issue of the following publications, which are generally available in most libraries: *Energy Research Abstracts, (ERA); Government Reports Announcements* and Index (*GRA* and I); *Scientific and Technical Abstract Reports (STAR);* and publication, NTIS-PR-360 available from NTIS at the above address.

SERI/STR-211-2923
UC Category: 63
DE86004449

MASTER

$CuInSe_2$ Solar Cell Research by Sputter Deposition

Annual Subcontract Report
1 December 1984 - 31 December 1985

J. A. Thornton
T. C. Lommasson
A. F. Burnett
University of Illinois
Urbana, Illinois

SERI/STR--211-2923

DE86 004449

April 1986

SERI Technical Monitor:
H. S. Ullal

Prepared under Subcontract No. XL-5-04131-1

Solar Energy Research Institute
A Division of Midwest Research Institute

1617 Cole Boulevard
Golden, Colorado 80401-3393

Prepared for the
U.S. Department of Energy
Contract No. DE-AC02-83CH10093

TABLE OF CONTENTS

LIST OF FIGURES AND TABLES

ABSTRACT

This report covers the period December 21, 1984 to December 31, 1985, with emphasis on the period July 1, 1985 to December 31, 1985. Research during the period December 21, 1984 to June 30, 1985 is described in a Semiannual Technical Progress Report dated July 31, 1985.

The project is based on work conducted at Telic Corporation, Santa Monica, California, during the period from June 1982 to October 1983. An in-line sputtering apparatus with a vacuum interlock and four deposition chambers configured for depositing $CuInSe_2/CdS$ heterojunctions by reactive sputtering without breaking vacuum was designed at Telic in 1983. In the Spring of 1984 the unit was moved from Telic to the University of Illinois. During the first phase of the present program the apparatus was installed in the Coordinated Science Laboratory with appropriate safety features for handling the hazardous gases, and shakedown test were conducted. In addition, characterization facilities were assembled at Illinois for measuring the cell current-voltage characteristics in the dark and under illumination, and for making spectral response, capacitance-voltage, and optical absorption coefficient and bandgap measurements.

Studies of the influence of the current to the Cu and In sources on the composition and resistivity of co-sputtered Cu-In-Se coatings were described in the semiannual progress report. Abrupt variations in resistivity with composition were found, consistent with the previous Telic work and with the observations on evaporated coatings. Stoichiometric coatings exhibited high resistivity ($> 5 \times 10^3$ Ω-cm). Coatings within the chalcopyrite phase field, on the In side of the stoichiometric composition, exhibited n-type conductivity. Coatings of the Cu-rich side of the stoichiometric composition were p-type. X-ray diffraction measurements have now confirmed that the Cu-rich coatings are a two-phase mixture of Cu_2Se and $CuInSe_2$. The desired p-type material appears to be found in a very narrow region on the In-deficient side of the stoichiometric composition. Indium sticking coefficients have been deduced from the compositions of coatings deposited at low ($\sim$ 50°C) and high ($\sim$ 400°C) substrate temperatures and concluded to be a sensitive function of the coating composition under typical deposition conditions. This exacerbates the task of composition control

and appears to be a factor in favor of the two-layer deposition procedure used for virtually all $CuInSe_2$ device fabrication using evaporated coatings.

Experiments have been conducted to investigate two-layer $CuInSe_2$ coatings formed by depositing an In-rich top layer over a Cu-rich two phase (Cu_2Se—$CuInSe_2$) base layer. Solid state reactions during deposition appear to yield a nearly homogeneous chalcopyrite material. Deposition conditions can be selected that consistently yield compositions within the range required for device fabrication. Devices with efficiencies in the 4-6% range were fabricated at the University of Delaware Institute of Energy Conversion from this material. A major thrust in our present work is toward the development of cell fabrication capabilities at Illinois using both reactive sputtered and evaporated CdS.

1. PROJECT DESCRIPTION

1.1 Overall Objection

The overall objective of this project is to develop a large area deposition technique and a concomitant high-efficient cell design for thin-film $CuInSe_2$. The program has two general objectives:

1) To conduct fundamental studies of the processes involved in the magnetron reactive sputtering of $CuInSe_2$ and associated materials, in order to provide knowledge of the type that would be required in a scaling of the process to the production quantities required for terrestrial applications.
2) To fabricate photovoltaic devices incorporating sputtered $CuInSe_2$ in order to identify problem areas and to demonstrate that sputtered material can indeed be used to form high-performance (over 10%-efficient) $CuInSe_2$ cells.

Sputtering, particularly using magnetron methods, offers great promise for depositing high quality films over large areas at the production volumes and low costs that will be required to make large scale terrestrial photovoltaic applications feasible. The program is of thirty months duration. The University of Delaware Institute of Energy Conversion (IEC) is working under subcontract to assist the University of Illinois in device fabrication and characterization until such time as suitable facilities to perform these functions can be established at Illinois.

1.2 Previous Work

The present program is based on work conducted at Telic Corporation in Santa Monica, California, during the period from June 1982 to October 1983.[1,2] A first preliminary phase of the Telic studies demonstrated that $CuInSe_2$ coatings having stoichiometric compositions (within the experimental accuracy of energy dispersive X-ray fluorescence measurements) could be deposited by reactive co-sputtering from Cu and In planar magnetron sputtering sources in an $Ar+H_2Se$ working gas.[1,3–6] X-ray diffraction measurements indicated that the stoichiometric coatings possessed a single phase chalcopyrite structure. The photovoltaic capabilities of homogeneous single layer coatings of the reactive sputtered $CuInSe_2$ were evaluated at IEC by evaporating CdS onto them to form $CuInSe_2$/CdS heterojunctions. Devices fabricated from these heterojunctions yielded $J_{SC} \sim 33$ mA/cm^2 (at 100 mW/cm^2), $V_{oc} \sim 0.25$, FF ~ 0.50 and efficiencies of about 4%.

The preliminary $CuInSe_2$ studies described above were conducted using sputtering equipment which had been originally designed to fabricate all-sputtered Cu_2S/CdS solar cells[1] and that was modified[1] to facilitate reactive co-sputtering from Cu and In planar magnetron sources. Two problems limited the effectiveness of this apparatus, which will subsequently be referred to as the radial apparatus. First, a lack of space within the deposition chamber necessitated placing the sputtering sources in locations such that the Cu and In deposition fluxes approached the substrates at oblique angles (about 35° off the normal) and produced significant variations in composition across the 25 mm wide substrates. Second, although the evidence was not conclusive, indications of cross-contamination were seen when the vacuum chamber was used sequentially with H_2Se and H_2S reactive gases to form all-reactive-sputtered $CuInSe_2/CdS$ heterojunctions. Accordingly, it was concluded that the use of this apparatus for attempts at detailed device optimization, or the fabrication of all-sputtered cells, was not warranted. However, the work with the radial apparatus did demonstrate that reactively sputtered $CuInSe_2$ could be deposited into forms suitable for application in $CuInSe_2/CdS$ solar cells.

The second phase of the Telic work involved the design and construction of an in-line deposition apparatus, with separate chambers for performing the $CuInSe_2$ and CdS reactive sputtering and with the $CuInSe_2$ deposition station configured to reduce the composition gradients described above[2]. See Figure 1. In October of 1983 Telic/Dart & Kraft decided to terminate its involvement in thin film research. In March 1984, the in-line deposition apparatus was moved to the University of Illinois. Facilities were prepared and the in-line apparatus was installed at the Coordinated Science Laboratory in the fall of 1984. The present program, which resumed the $CuInSe_2$ reactive sputtering studies at the University of Illinois, was begun in January of 1985.

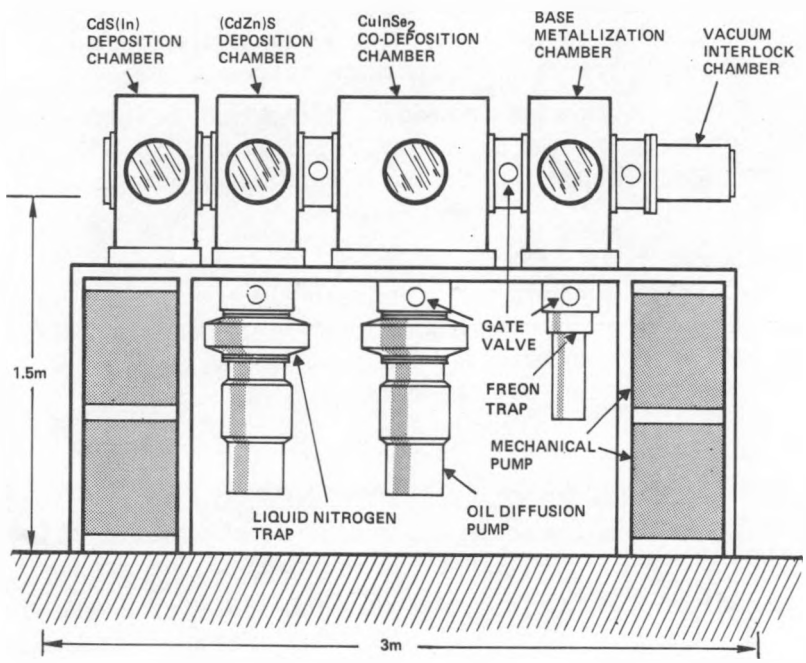

Fig. 1. Schematic drawing of in-line sputtering apparatus configured for fabricating $CuInSe_2$ heterojunctions.

1.3 Summary of Work Statement

Task 1: *Development of Characterizaton Capability*

Suitable instrumentation shall be acquired, and a competence shall be developed for making --

1) I-V characterizations of solar cells in the dark and under simulated AM1 illumination.
2) Measurements of cell quantum efficiency as a function of wavelength, both with and without light bias.
3) C-V characterizations of heterojunctions, in the dark, under AM1 illumination, and as a function of the spectral content of the bias light.

In addition, calibration measurements shall be made to adapt an x-ray fluorescence system at the University of Illinois at Urbana-Champaign for making composition measurements of $CuInSe_2$ and of CdS doped with In.

Task 2: *Apparatus Shakedown* and *Scaling Studies*

1) A shakedown of the in-line sputtering apparatus shall be performed by depositing $CuInSe_2$ coatings and fabricating hybrid cells, incorporating evaporated CdS.
2) Deposition data obtained during the shakedown studies shall be compared with data obtained with the radial apparatus in order to gain an improved understanding of the geometric and scaling effects associated with the $CuInSe_2$ reactive-sputtering processes.

Task 3: *$CuInSe_2$ Reactive Sputtering Process*

Fundamental studies shall be conducted to elucidate the basic reactive-sputtering mechanisms that are operative in the deposition of materials such as $CuInSe_2$ using working gases such as H_2Se. Particular attention shall be given to substrate reactions, such as the one which apparently results in the release of volatile In-Se species, and the influence of these reactions on the properties of the resultant coatings.

Task 4: *Optimization of All-Sputtered $CuInSe_2$/CdS Solar Cells*

The objective of this task shall be to begin a systematic investigation of the *in situ* fabrication of all-sputtered $CuInSe_2$/CdS solar cells using the in-line system. The task shall include:

1) Investigating the effects of the $CuInSe_2$ electrical and optical properties and thickness on the performance of all-sputtered $CuInSe_2$/CdS cells. Particular attention shall be given to the use of uniform and graded compositions with the $CuInSe_2$ layers.
2) Investigating the effect of the relative resistivity of the $CuInSe_2$ and CdS layers on the performance of all-sputtered $CuInSe_2$/CdS solar cells.
3) Investigating cells in which the CdS is replaced by (CdZn)S for the purpose of increasing the cell open-circuit voltage.
4) Comparing the effectiveness of alumina and borosilicate glass as substrates for all-sputtered $CuInSe_2$/CdS solar cells.

Task 5: *Evaporated CdS*

A vacuum chamber shall be assembled, and suitable sources shall be installed in the chamber, to permit the deposition of indium-doped CdS coatings by co-evaporating CdS powder and elemental In. These coatings will be used in the fabrication of hybrid cells incorporating sputtered $CuInSe_2$ and evaporated CdS. This chamber will also incorporate provisions for evaporating aluminum top grid electrodes in support of the cell fabrication activities.

Task 6: *Testing of Hybrid Sputter–Evaporation System*

The in-line deposition apparatus shall be modified to permit co-deposition by evaporating Se and sputtering Cu and In. Preliminary studies shall be made in which $CuInSe_2$ films are deposited by this hybrid method and tested by $CuInSe_2$ cell fabrication.

Task 7: *Thin Film Drift–Field Cell*

A p-i-n type device, with a very thin (100 to 500 nm) $CuInSe_2$ "intrinsic" layer of relatively high resistivity, shall be fabricated. The approach shall be to establish a strong electric field in the $CuInSe_2$ absorption layer, so that the high absorptivity of the $CuInSe_2$ can be taken advantage of in a configuration that might make the cell performance relatively insensitive to the $CuInSe_2$ material properties. This could widen the deposition condition "window" for obtaining high-performance devices. The other advantage of a thinner cell would be lower production cost, which would result from the reduced deposition time and reduced amount of indium required.

Task 8: *Reactively Sputtered $Cu(In,Ga)Se_2$ Alloy*

The deposition of $Cu(In,Ga)Se_2$ alloy coatings by reactive sputtering using alloy metal targets and Ar-H_2Se as a working gas shall be investigated. The experiments shall be conducted using a Ga composition that is about 30% of the In composition. The electrical and optical properties of the resultant films shall be determined. Preliminary cells shall be fabricated using the reactive sputtered $Cu(In,Ga)Se_2$ layers.

Task 9: *Cell Stability Testing*

Cells with efficiencies greater than 4% shall be set aside, stored in air, and subjected to periodic performance testing under illumination in order to begin to accumulate data on the stability of sputtered $CuInSe_2$ cells. Cells shall be supplied to SERI for stability testing at SERI's request.

Task 10: *Study of High–throughput Sputter–Deposition of $CuInSe_2$*

The process of fabricating $CuInSe_2$/CdS cells by reactive magnetron sputtering shall be analyzed for the purpose of investigating its potential for being scaled to high-throughput systems.

Task 11: *Device Characterization and Fabrication*

A subtier subcontract shall be negotiated with the University of Delaware, Institute of Energy Conversion (IEC), to provide support in the accomplishment of Tasks 1, 2, 4, 5, 7, 8, and 9 above.

a) The IEC characterization of the sputter-deposited $CuInSe_2$ will include but not be limited to

- Measurements of the resistivity, Hall mobility, and charge carrier density.
- Measurements of the optical bandgap and optical absorption coefficient.
- X-ray diffraction determinations of the crystallographic phases present.
- EDAX measurements to determine the film composition.

b) The $CuInSe_2$/CdS cell characterization will include but not be limited to

- Laser scan measurements of the uniformity of the photovoltaic response.
- I-V characterization of solar cells in the dark and under AM1 illumination.
- C-V characterization of heterojunctions in the dark, under AM1 illumination, and as a function of the spectral content of the light.
- Measurement of cell quantum efficiency as a function of wavelength, both with and without light bias.

c) Additional activities at IEC in support of the sputtering effort will include but not be limited to

- General consulting on cell fabrication and performance.
- Deposition of top grid electrodes.
- Testing of cells set aside for stability observations.
- Deposition of evaporated CdS onto sputtered $CuInSe_2$ layers supplied by Telic, to yield hybrid heterojunctions suitable for evaluating the photovoltaic properties of the sputtered $CuInSe_2$.

1.4 Project Status

The tasks of developing a cell characterization capability (Task 1) and conducting shakedown tests for the in-line sputtering apparatus (Task 2) have been completed and were discussed in detail in the semiannual report.[7]

The major emphasis during our fundamental reactive sputtering studies (Task 3) has been on developing an improved understanding of two factors that introduce a nonlinear behavior into the relationship between the currents delivered to the Cu and In sputtering sources and the composition of the resultant coatings. The first is the formation of surface layers of modified composition on the target surfaces. The second is the variation of the coating atom sticking coefficients (particularly In and Se) with the surface composition of the growing coating.

The formation of cathode surface layers, and their influence on the temporal response of the deposition system during changes in the currents to the sputtering sources, was discussed in the Semiannual Report. Although a surface layer sufficient to modify the sputtering yield from the In target appeared to form, it was too thin to influence the time response of In sputtering rate to changes in the discharge current. In the case of the Cu cathode a surface layer having the nominal composition of copper selenide (Cu_2Se) formed with thicknesses sufficient to make the sputtered Cu flux sluggish in its response to changes in the discharge current. Therefore variations in the current to the In source, at fixed currents to the Cu source, were used to investigate the influence of the sputtering currents on the composition and resistivity of the resultant coatings during the shakedown tests of the in-line apparatus which were conducted at Illinois. These experiments, which were described in the semiannual report, provided a much more detailed picture of the resistivity

variations across the $CuInSe_2$ chalcopyrite phase field than was possible in the previous Telic experiments and showed the abrupt variations in both resistivity and composition with deposition flux that have also been reported for evaporated coatings.[8–11] The stoichiometric coatings exhibited the expected high resistivity ($> 5 \times 10^3$ Ω-cm). Coatings within the chalcopyrite phase field, which extends on the In-rich side of the stoichiometric composition, exhibited n-type conductivity with a resistivity of about 10^3 Ω-cm. Coatings on the Cu-rich side of the stoichiometric composition were p-type, with resistivities which decreased with increasing Cu content, and were as low as 10^{-1} Ω-cm for coatings with the nominal composition: Cu-30 at. %, In-20 at. %, Se-50 at. %. X-ray diffraction measurements have now confirmed that the Cu-rich coatings are a two-phase mixture of Cu_2Se and $CuInSe_2$, as one would expect from the phase diagram.

Measurements of the relative In and Se sticking coefficients show that they are dependent on the composition of the growing film surface. Evidence of a similar behavior has recently been reported for evaporated coatings by a group in Sweden.[10,11] This dependence is believed to be a major factor in explaining the nonlinear relationship between the coating composition and the deposition flux.

It appears that much of the difficulty associated with the nonlinear dependence of coating composition on the composition of the incident sputtered or evaporated fluxes can be avoided by depositing Cu-rich and In-rich Cu-In-Se layers and forming the desired $CuInSe_2$ coating by a solid state reaction between the two layers. This Boeing two-layer approach[12] appears to have been used for all of the higher efficiency $CuInSe_2$/CdS devices fabricated to date. Accordingly, two-layer reactively sputtered $CuInSe_2$ coatings, deposited at 400°C using various layer combinations, have been investigated. The experiments indicate almost total mixing between the two layers and show that device quality $CuInSe_2$ can be obtained using starting layer compositions that are significantly different from those normally used.[13] It is also found that the composition of the resultant composite coating can be controlled to within about 0.5 at. % without feedback control by simply fixing the reactive sputtering conditions.

$CuInSe_2$/CdS devices have been fabricated at the University of Delaware Institute of Energy Conversion by combining sputtered $CuInSe_2$/Mo layers prepared at Illinois with evaporated In-doped CdS layers (Task 4). In the previous work at Telic, adhesion problems were encountered at the $CuInSe_2$/Mo interface when smooth glass or polished alumina substrates were used. A change in the deposition procedure to minimize the Se concentration at the interface appears to have overcome this difficulty, as was discussed in the semiannual report. Most of the cell fabrication thusfar has been done using two-layer $CuInSe_2$ coatings in which the Cu-rich base layer was considerably richer in Cu (Cu ~ 30 at. %, In ~ 20 at. %, Se ~ 50 at. %) than that used by most groups. A cell efficiency of 5.5% has been achieved. However, future cell fabrication work will concentrate on using $CuInSe_2$ composite layers in which the base layer compositions are less rich in Cu and more in the range used by other groups (Cu ~ 25.5 at. %, In ~ 24.5 at. %, Se ~ 50 at. %) in order to avoid a rough surface topography encountered in the Cu-rich layers. The cell fabrication work revealed that, although the in-line apparatus was far superior to the Telic radial apparatus in removing composition gradients at the substrate, variations in material properties sufficient to influence the device behavior were present. Therefore shields have been added to reduce these gradients.

A major thrust in our present work is toward the development of a photovoltaic device fabrication capability within the Thin Film Physics Group at Illinois. CdS layers will be deposited by reactive sputtering, using the in-line apparatus, and by evaporation. A chamber has been prepared for use in co-evaporating CdS and In to form coatings of In-doped CdS (Task 5). Evaporation sources for the CdS and In are of the same type that have been used effectively at IEC. The chamber also has provisions for forming top grid electrodes by evaporating Al through magnetically-held-down Kovan deposition masks. The initial cell configuration will be similar to that used by IEC and will use photolithograph methods to pattern the $CuInSe_2$ and CdS and thereby to form an array of twelve 3 mm x 3 mm cells on the $CuInSe_2$/Mo substrates. An ultrapure water system, with provisions for substrate cleaning and rinsing, has been installed to reduce the number of substrate-contamination-induced pinhole problems in anticipation of fabricating devices with thinner $CuInSe_2$ layers (Task 7).

2. DEVELOPMENT OF CHARACTERIZATION FACILITY

The designs of characterization facilities for measuring the cell current-voltage characteristics in the dark and under illumination and for making spectral response and capacitance-voltage measurements were discussed in the semiannual report. The cell I-V system is controlled by an HP 3817 desktop computer operating through an HP 3497 data acquisition and control unit. Simulated light is provided by a single ELH lamp which will be calibrated by the current output from a $CuInSe_2$ reference cell provided by SERI, so that cell efficiency measurements can be made.

The spectral response system uses light from a 300 W tungsten halogen lamp which is passed through a 1/4 m Kratos monochromator and is controlled by the HP computer and data acquisition unit. The system is capable of covering the wavelength range from 400 nm to 1800 nm. Bias light is provided from an ELH lamp.

The capacitance-voltage measurements are made with an HP 4275A LCR meter which is controlled by the HP computer and data acquisition unit. Measurements can be made over the frequency range from 100 Hz to 100 kHz, with or without bias light.

A photothermal deflection system is being constructed on another program will also be available for making sub-bandgap absorption measurements.

A Perkin Elmer Lambda 9 double beam spectrometer with an integrating sphere and computer control has been provided for use on the program by the University of Illinois. The computer is being programmed to make absorption coefficient and optical bandgap determinations from total reflectance and transmission measurements. The spectrometer is capable of making reflectance and transmission measurements over the wavelength range from 200 nm to 2500 nm. A tungsten halogen lamp is used as a light source for the visible and near infrared range and a deuterium lamp is used for the ultraviolet range. The lamp output is passed through a double monochromator system that provides a sample beam (S) and reference beam (R) at the measurement chamber shown schematically in Fig. 2. The detector is a 60 mm integrating shere which contains a photomultiplier and a PdS cell. The spectral range of the integrating sphere is from 200 nm to 2500 nm. When

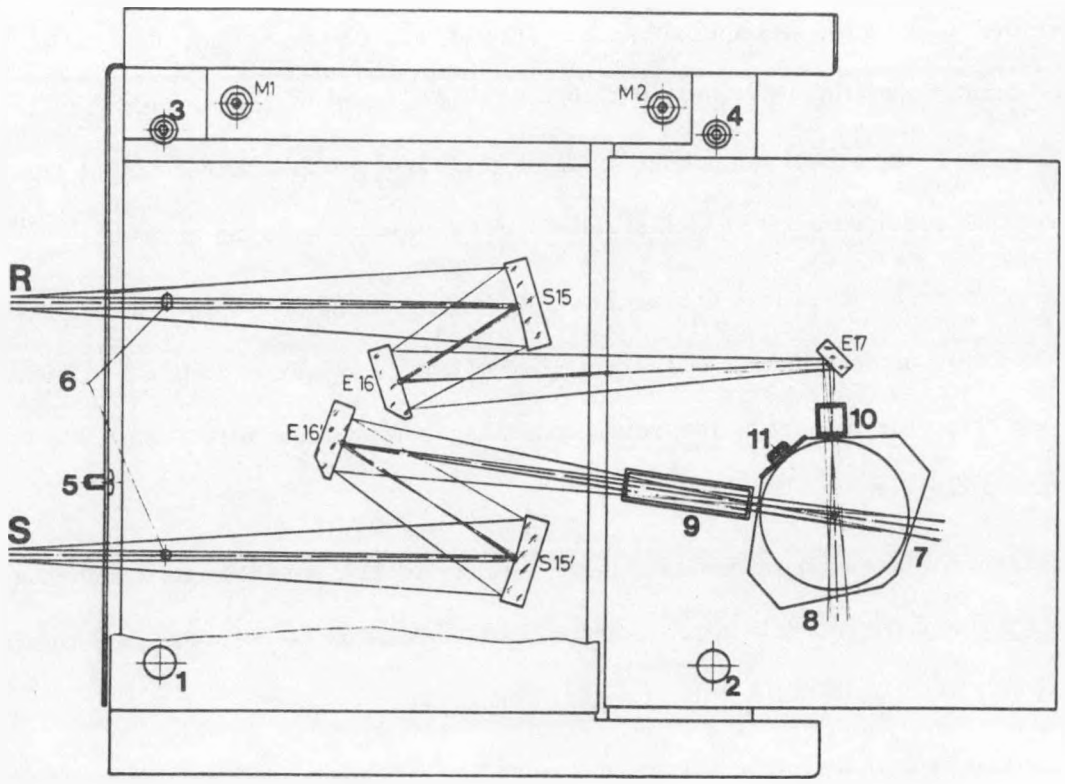

Fig. 2. Schematic drawing of integrating sphere measurement chamber on Perkin Elmer Lambda 9 double beam spectrometer. R is reference beam, S is sample beam, 7 is reference sample port, 8 is reflectance reference port, 9 is transmission sample port, 10 is transmittance reference port and 11 is specular component aperture.

percent transmission is to be measured, the sample is placed at position 9 and a reference is at position 10. All light passing through the sample is collected by the integrating sphere and measured. The sample and reference beams are chopped and monitored alternately. This removes any sensitivity to drift in the detector performance. When percent reflectance is to be measured the sample is placed at position 7. Either the total reflectance or the diffuse reflectance can be measured. The specularly reflected light from position 7 falls at position 11. If a reflector is at position 11 the light stays in the integrating sphere and total reflectance is measured. If a light trap is at position 11, the specular component of the reflected light is removed from the sphere and only the diffuse reflection is measured.

3. APPARATUS SHAKEDOWN AND SCALING STUDIES

The shakedown tests of the in-line sputtering apparatus were described in detail in the semi-annual report. At that time the apparatus and the substrate manipulation system had functioned properly for about 200 deposition runs. The system has now functioned for over 500 runs without malfunction.

One significant modification has been made to the in-line apparatus since the semiannual report was prepared. This involved the installation of deposition shields to reduce the composition gradient at the substrates. Variable angles of incidence and composition gradients are unavoidable when co-depositing from large area sources onto stationary substrates. The problem has been minimized in co-evaporating $CuInSe_2$ coatings by using small area sources placed a considerable distance from the substrates. The problem is avoided in in-line production sputtering machines by continuously moving the substrates past long magnetrons which act essentially as line sources of coating material. Composition variations across the substrate width were a severe problem in the early Telic reactive sputtering work because the lack of space within the deposition chamber had necessitated placing the substrates close to the sources (about 90 mm) at positions such that the coating fluxes approached the substrates at significantly oblique angles (about 35° off the normal). One of the objectives in the design of the in-line apparatus was to reduce these composition gradients. This was done by increasing the source-to-substrate distance to 228 mm. This reduced the average angle of incidence to about 22 1/2° and left room to add shields which could further improve the uniformity and reduce the angle of incidence to about 12°. Data showing effectiveness of the in-line configuration was given in the semiannual report.[7] The composition variation across a 16 mm wide region in the center of a 25 mm wide substrate was reduced from over 10% to about 4% for pure Cu and In co-deposited at room temperature.

A 4% composition variation would obviously be unacceptable for $CuInSe_2$ device fabrication. However, when Cu-In-Se coatings with In-rich compositions within the chalcopyrite phase field were deposited, the composition variations were much less. Thus data was presented in the semian-

nual report for a Cu-In-Se coating with the nominal composition (Cu - 23 at. %, In - 27 at. %, Se - 50 at. %) deposited at 400°C. The composition variation over the center 16 mm region of the substrate was less than 1%. This behavior, which was first observed in the Telic reactive sputtering work,[3–5] is a consequence of the tendency for surface reactions to reject excess In during film growth and thereby to promote the formation of near-stoichiometric deposits. See Section 4. Similar behavior apparently occurs during $CuInSe_2$ deposition by co-evaporation. Thus Baron has recently reported relatively uniform composition and device performance over 10 cm x 10 cm substrates for films deposited by co-evaporation using an apparatus in which the Cu/In flux is predicted to vary over the substrate surface by as much as 20 to 30%.[14] Therefore it was decided at the time of the initial shakedown experiments that no additional shielding would be added until a clear need was established, since the shields do cause about half of the sputtered flux to be lost.

Unfortunately, as one might expect, the composition smoothing behavior described above occurs only on the In-rich side of the stoichiometric composition. When we began depositing two-layer $CuInSe_2$ films from Cu-rich base layers and In-rich top layers (see Section 4), variations in the composition of the base layer were encountered that were sufficient to influence the performance of devices fabricated from the composite $CuInSe_2$ layers (see Section 5). Therefore toward the end of this reporting period additional shielding was added to the $CuInSe_2$ deposition chamber of the in-line apparatus. The configuration of the shields are shown in Figure 3. The shields effectively reduced the size of the deposition sources by a factor of about two and the average angles of incidence to about 10°. Figure 4 shows a measurement of the composition uniformity across the substrate surface for co-sputtered Cu/In coatings deposited with and without the shields. The measurements were made at SERI by X-ray fluorescence using a wavelength dispersive spectrometer with an accuracy of about ± 0.4%. The shields are seen to have reduced the concentration variation across the essential width of the substrate by a factor of about four. It is important to re-emphasize that the shields described above were added at the end of the reporting period. Thus the data that is reported in Sections 4 and 5 was obtained before the shields were installed.

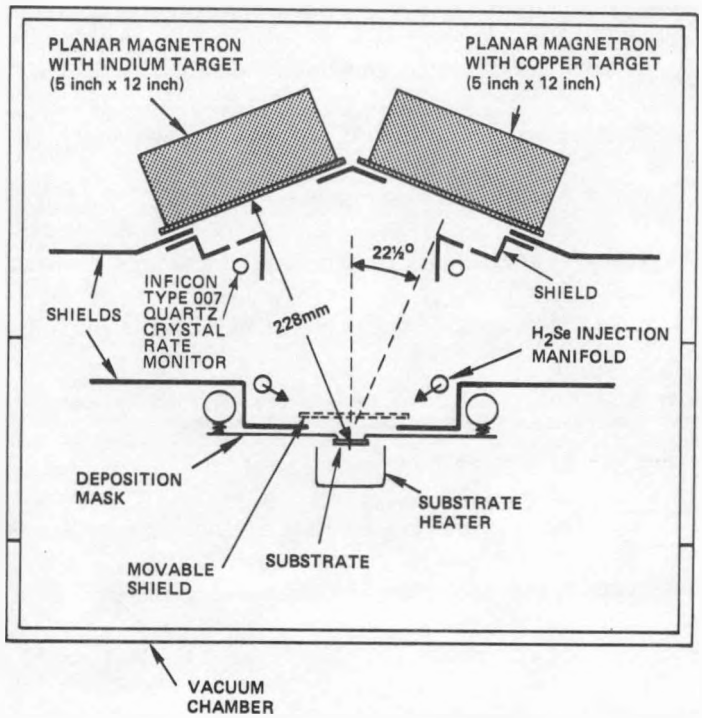

Fig. 3. Plan view illustration of $CuInSe_2$ co-deposition chamber showing position of new deposition shields that have been added to improve the composition uniformity at the substrate plane. The location of quartz cyrstal rate monitors behind the sheidls is also shown.

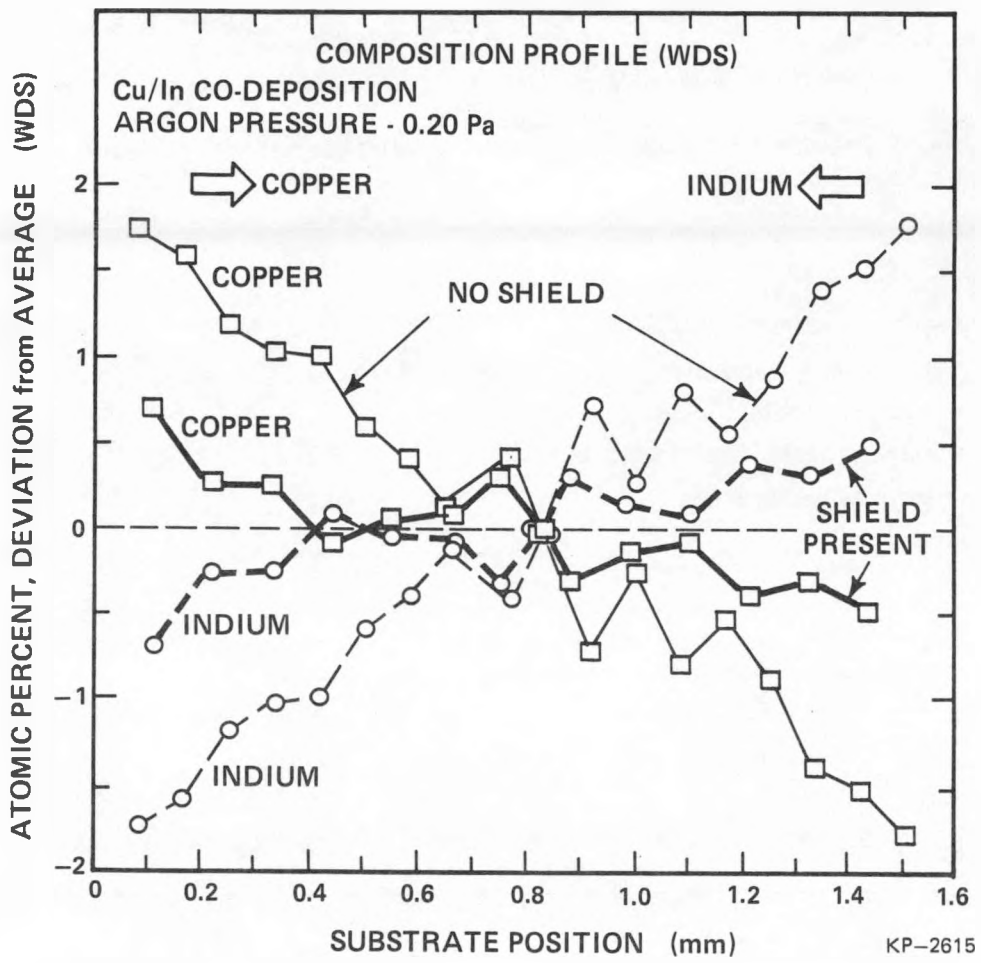

Fig. 4. Composition uniformity across the substrate surface for copper/indium films, that were co-sputtered in the $CuInSe_2$ deposition chamber, showing the effect of the new deposition sheilds.

Two additional modifications are also being made to improve our ability to monitor and control the deposition process in the in-line apparatus. Inficon type 007 quartz crystal microbalance deposition rate monitors are being added as shown in Figure 3 to provide independent measurements of the sputtered fluxes from the Cu and In targets. A Molytex Model 3702 thirty two channel data logger, operated through an IBM portable PC microcomputer, has been added to monitor and record process parameters during the reactive sputter deposition. Parameters of interest include:

- Discharge current to copper source,
- Discharge voltage at copper source,
- Discharge current at indium source,
- Discharge voltage at indium source,
- Substrate temperature,
- Power to substrate heater lamp.
- H_2Se flow rate,
- Ar flow rate,
- Total system pressure,
- Pressure change due to reactive gas consumption,
- Sputtering rate from copper source,
- Sputtering rate from indium source.

Finally, movable masks have been installed in the Cu-In-Se deposition chambers, and a stationary mask was installed in the Moly base layer chamber. By using these masks in various combinations, it is now possible to isolate areas with the following coating configurations on a single substrate.

- $CuInSe_2$ base layer on glass.
- $CuInSe_2$ base layer on Mo.
- $CuInSe_2$ top layer on glass.
- $CuInSe_2$ top laer on Mo.
- Composite two-layer $CuInSe_2$ coating on glass.
- Composite two-layer $CuInSe_2$ coating on Mo.

The use of two-layer composite $CuInSe_2$ coatings is discussed in Section 5.1.

4. $CuInSe_2$ REACTIVE SPUTTERING PROCESS

4.1 The Cu-In-H_2Se Reactive Sputtering Process

As a general rule, significant reactions occur in the plasma and at the target as well as on the substrate (chamber wall) surfaces during reactive sputtering. The Cu-In-H_2Se reactive sputtering process is shown schematically in Fig. 5. The injected H_2Se molecules may be directly incident on the substrate surface or they may pass through the plasma, where electron-molecule collisions can produce dissociation and/or ionization. The molecules or their products may eventually reach the target surface where their interaction can be further stimulated by the ion bombardment. The result may be the formation of a surface layer of modified composition on the target surface. The nature of such a surface layer is dependent on a balance between its rates of formation and removal, and therefore on the magnitude and composition of the ion flux as well as those neutral fluxes that carry reactive species to the target surface. The steady sputtered flux leaving the target is therefore often the consequence of the sputtering of such a surface layer.

Our knowledge of the details of the Cu-In-H_2Se reactive sputtering process is sketchy at best. Our approach is therefore to accumulate information on the process from observations made while conducting semi-empirical experiments to optimize film properties and from special experiments designed to elucidate particular mechanisms in greater detail. Following is a brief summary of our current state of understanding.

Modified Surface Layers on Target. Under the typical operating conditions that have been used to produce stoichiometric $CuInSe_2$ coatings, modified surface layers form on both the Cu and In sputtering targets. The effective partial sputtering yields, defined as the number of sputtered metal atoms per incident ion, were measured and found to be about 0.7 atoms/ion for the Cu target and 0.5 atoms/ion for the In target.[4] These values can be compared with the elemental yields of about 2 Cu atoms/ion and 3 In atoms/ion respectively for Ar sputtering from clean Cu and In surfaces. The modified surface on the Cu target has the nominal composition of Cu_2Se and could be as much as a micron thick.[4,7] The modified surface layer on the In target is too thin to be detected by

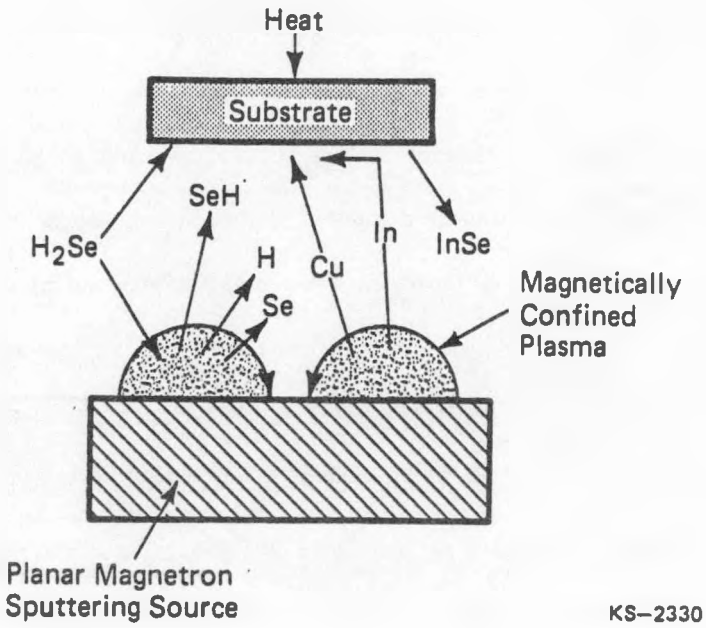

Fig. 5. Schematic illustration of Cu-In-H_2Se reactive sputtering process. The evolution of InSe from the target is suggested by experimental observations but has not been proven. See Ref. 7.

collecting and analyzing the material sputtered from the surface in pure Ar.[7]

Total Fluxes. H_2Se injection rates under the operating conditions that have been used to produce stoichiometric coatings are typically about 60 Pa-liters/sec (1.6×10^{19} molecules/sec). Total metal atom sputtering rates from the Cu and In targets can be estimated from the effective sputtering yields cited above. For a current of 0.7A to the Cu source and 1.0A to the In source the fluxes are $(0.7)(0.7)/(1.6 \times 10^{-19}) = 3 \times 10^{18}$ Cu-atoms/sec and $(0.5)(1.0)/(1.6 \times 10^{-19}) = 3 \times 10^{18}$ In-atoms/sec, where we have neglected the effect of the secondary electron currents in calculating the ion fluxes. The total consumption of H_2Se, estimated from absolute pressure and mass spectroscopy measurements, is typically about 2/3 of the injected flux or 40 Pa-liters/sec (10^{19} molecules/sec).[4] The flux of consumed H_2Se is indeed seen to be about equal to the flux of 6×10^{18} molecules/sec that would be required to convert the sputter metal fluxes into $CuInSe_2$.

Surface Impingement Rates. Partial pressure measurements of the stable molecular species involved in the reactive sputtering process have been made using a quadruple mass spectrometer calibrated with an capacitive manometer.[4] Under typical operating conditions the partial pressures were Ar $\sim$ 0.2 Pa, $H_2Se \sim$ 0.3 Pa, and $H_2 \sim$ 0.1 Pa. The estimated surface impingement rates are then Ar $\sim 7 \times 10^{17}$ atoms/cm^2-sec, $H_2Se \sim 5 \times 10^{17}$ molecules/cm^2-sec, and $H_2 \sim 1.5 \times 10^{18}$ molecules/cm^2-sec. The metal flux impingement rates at the substrate (based on deposition flux collected on room temperature substrates) are typically about 10^{15} Cu atoms/cm^2-sec and 1 to 4×10^{15} In atoms/cm^2-sec, depending on the deposition conditions. The ion fluxes in the intense sputtering regions of the planar magnetron sources (estimated to be 50 cm^2 in size) are about 10^{17} ions/cm^2-sec for a typical discharge current of 1A.

H_2Se Substrate Interaction. The impingement rates of both H_2Se and H_2 on the substrate surface are seen above to be higher than that of the arriving metal flux by a factor of 10^2 or more. The decomposition temperature for H_2Se is about 160°C. Therefore, one might speculate that the surface of the substrates, which are typically maintained at 400°C, is covered with at least a fraction of a monolayer of Se which may in fact be in equilibrium with the H_2Se in the gas phase.

However, no visual evidence of a surface interaction was seen when 150 nm thick Cu-In coatings were exposed at 400°C to an H_2Se impingement flux of $\sim 5 \times 10^{17}$ molecules/cm^2-sec for 15 minutes.[7]

Plasma Volume Interaction. There is evidence[15] that the excited electronic states in the H_2Se molecule have a great deal of antibonding character and, therefore, most electron impact excitation events will lead to dissociation according to the reaction $H_2Se + e^- \rightarrow SeH + H + e^-$. Based on the H_2S mass spectroscopy cracking pattern,[16] we expect the plasma to include H_2Se^+, HSe^+, Se^+, and H^+ ions. Thus these ions, as well as Ar^+ and SeH radicals, are expected to be incident on the cathode surface. Assuming a total inelastic electron cross section of 10^{-16} cm^2 for electron-H_2Se collisions, an electron density of 10^{11} cm^{-3} and an average energy of 10 eV in the magnetron plasma, and a H_2Se partial pressure of 0.3 Pa, gives an overall inelastic collision rate of about 10^{18} collisions/cm^3-sec. The magnetron plasma volumes are relatively small, being typically of the order of 50 cm^3 with a surface area of about 100 cm^2. Thus the H_2Se flux passing into the plasma volumes is $\sim 5 \times 10^{19}$ molecules/sec and the total inelastic collision rate within the plasma volumes could be of the order of 5×10^{19} molecules/sec. These fluxes are consistent with the total ion flux embodied in the magnetron discharge currents which is about 2×10^{19} ions/sec. The H_2Se gas exchange time for the deposition chamber (τ = chamber volume divided by H_2Se pumping speed) is about 2 sec. Thus the injected H_2Se molecules (rate $\sim 2 \times 10^{19}$ molecules/sec) have a reasonable probability of passing through the magnetron plasma during their stay in the chamber, and if they do pass into the plasma they have a good chance of being dissociated and/or ionized. This is consistent with the observation that about 2/3 of the injected molecules appear to be consumed by the reactive sputtering process.[4]

Target Surface Reactions. As noted previously, the ion flux in the intense sputtering regions of the planar magnetron sources is about 10^{17} ions/cm^2-sec. The impingement rate for H_2Se species is about 5×10^{17} molecules/cm^2-sec for all the surfaces in the chamber. However, the H_2Se species reaching the sputtering regions must pass through the magnetron plasma. The estimates of the

preceding section suggest that these molecules have a significant probability of being dissociated or ionized during this traverse. Therefore we expect the impingement rate of Se-containing radicals and ions on the target surface to be comparable to that of the Ar^+ ions. Therefore it is reasonable that selenide surface layers should form on both the Cu and In targets.

Gas Phase Reactions. Atomic hydrogen can attack H_2Se via a very rapid abstraction reaction of the form $H + H_2Se \rightarrow H_2 + SeH$.[17] If we assume that a total atomic hydrogen flux of 10^{19} atoms/sec leaves the magnetron plasma region and passes into the volume between the magnetrons and the substrate plane ($\sim$ 4000 cm^3), where it interacts with H_2Se at a partial pressure of 0.2 Pa, we obtain a total SeH production rate of about 19 radicals/sec for a gas kinetic cross section of 10^{-15} cm^{-2}. Thus, it appears that gas phase reactions of the hydrogen abstraction type cannot be ruled out as a source of Se radicals.

The above discussion suggests that our overall understanding of the Cu-In-H_2Se reactive sputtering process is self-consistent, although the details of the individual processes are in question and need to be addressed in special experiments. However, we do expect the impingement flux at the substrate surface to include H_2Se molecules from the working gas, SeH, H and H_2 molecules from the plasma, and high velocity Cu, In and Se sputtered species. Table 1 summarizes the various rates estimates included in the above discussion.

4.2. Experiments to Determine Film Properties as a Function of In/Cu Current Ratio

Figure 6 shows coating resistivity data obtained in a series of experiments conducted at a various currents to the In source, with a fixed current of 0.7A to the Cu source, injection rate of 75 Pa-liters/sec, and substrate temperature of about 400°C.[7] The substrates were Corning type 7059 glass plates. The coatings were deposited without the shielding shown in Fig. 3. The resistivities were calculated from coating thickness measurements that were made using a stylus instrument, and resistance measurements that were made by the four point probe method on small isolated regions of the coating at the center of the substrates. The isolated regions were in the form of

TABLE 1

Summary of rate parameters for Cu-In-Se reactive sputtering under typical conditions* that produce stoichiometric $CuInSe_2$ coatings

H_2Se injection rate -- 1.6×10^{19} molecules/sec.
Effective partial sputtering yield for Cu target - 0.7 atoms/ion.
Effective partial sputtering yield for In target - 0.5 atoms/ion.
Total flux of sputtered Cu atoms - 3×10^{18} atoms/sec.
Total flux of sputtered In atoms - 3 to 6×10^{18} atoms/sec.
Flux of H_2Se consumed in reactive sputtering process - 10^{19} molecules/sec.
Estimated total rate of electron - H_2Se inelastic collisions in magnetron plasma - 5×10^{19} molecules/sec.
Estimated total rate of H-H_2Se abstraction reactions $\sim 10^{19}$/sec.
Impingement rate of H_2Se species on chamber surfaces - 5×10^{17} molecules/cm^2-sec.
Impingement rate of Ar species on chamber surfaces - 7×10^{17} atoms/cm^2-sec.
Impingement rate of H_2 species on chamber surfaces - 1.5×10^{18} molecules/cm^2-sec.
Arrival flux of sputtered Cu atoms at substrate - 10^{15} atoms/cm^2-sec.
Arrival flux of sputtered In atoms at substrate - 1 to 2×10^{15} atoms/cm^2-sec.
Ion flux at target surface $\sim 10^{17}$ ions/cm^2-sec at 1A.

* Typical deposition conditions
H_2Se injection rate - 60 Pa-liters/sec
Ar pressure - 0.2 Pa
H_2Se pressure - 0.2 Pa
H_2 pressure - 0.1 Pa
Current to Cu source - 0.7A
Current to In source - 0.7 to 1.6A
Substrate temperature - 400°C

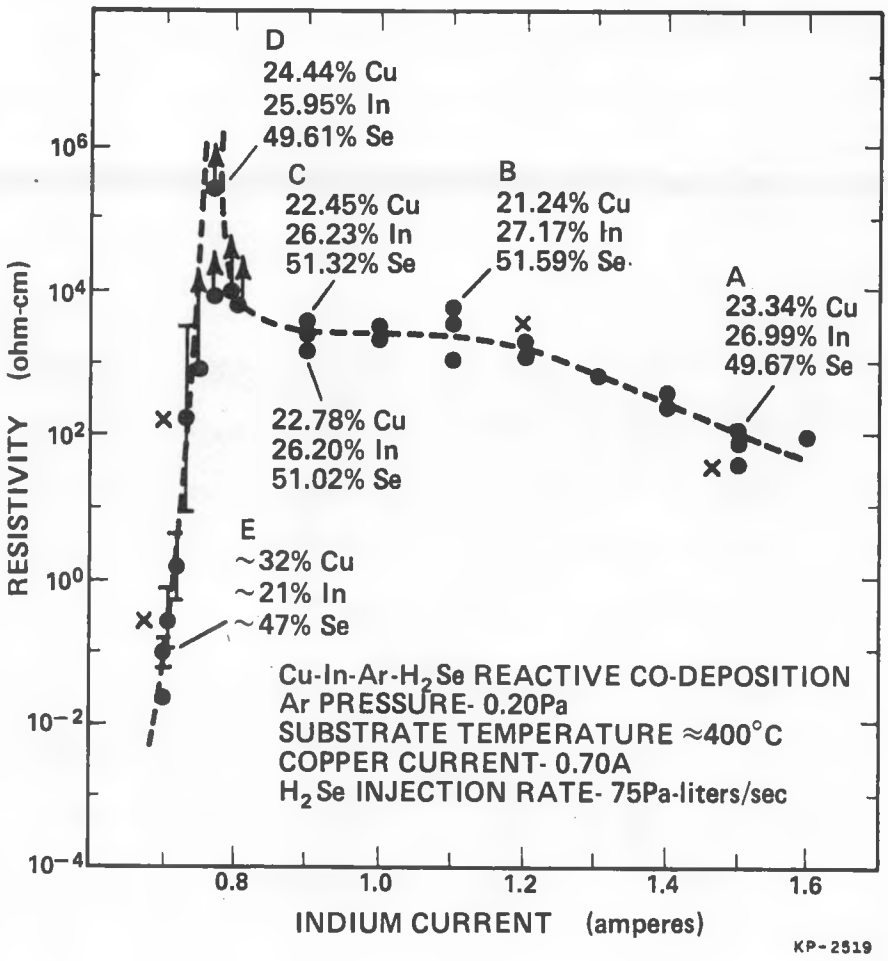

Fig. 6. Resistivity of reactive co-sputtered Cu-In-Se coatings versus current to In source for fixed current of 0.7A to Cu source, injection rate of 75 Pa-liters/sec and substrate temperature of 400°C.

strips, that were defined by scribing lines across the substrate with a razor blade, and were oriented perpendicular to the composition gradient discussed in Section 3. The composition data were determined at SERI by X-ray fluorescence, using a wavelength dispersive spectrometer with an accuracy of about ± 0.4%.

Figure 7 shows a pseudobinary phase diagram for the Cu_2Se—In_2Se_3 system.[18] The extent of the γ phase field is not known precisely, but in such material it is always observed on the side of the trivalent element (In^{+++} in our case) and never beyond the stoichiometric limit when the univalent element is in excess.[19] The dashed line in Fig. 7 corresponds to an atomic composition of about 23% Cu, 26% In and 51% Se.

Referring to Fig. 6, the maximum value of the resistivity is not known because of limitations in our instrumentation. However, we do know that it is greater than 4×10^5 ohm-cm for material with the composition Cu = 24.44 at. %, In = 25.95 at. % and Se = 49.61 at. %. Hot probe measurements indicate that the material on the Cu-rich side of the resistivity peak is p-type, that material at the peak is intrinsic, and the material on the In-rich sides is n-type. Thus, it is believed that the Fermi level can be envisioned as continuing to rise from a position near the valence band in the Cu-rich region, through the mid-gap positions at the resistivity peak, and finally into the vicinity of the conduction band in the In-rich region.

It is tempting to relate the resistivity peak shown in Fig. 6 to the stoichiometric boundary of the phase diagram. The In-rich material to the right of the peak, with resistivities in the 10^3 Ω-cm range, would then correspond to the γ-phase field shown in Fig. 7. X-ray diffraction has been used to study the crystallographic phases that are present in the material deposited on both sides of the resistivity peak. The material on the Cu-rich side appears to consist of a two-phase mixture of Cu_2Se and $CuInSe_2$ as implied by the phase diagram. Figure 8 shows the peak intensity of the Cu_2Se 030 line as a function of the Cu/In concentration ratio for the two phase Cu-rich material. The data is consistent with the expected decrease in the Cu_2Se component as one approaches the $CuInSe_2$ phase boundary. Similarly, the X-ray observations indicate that the material on the In-

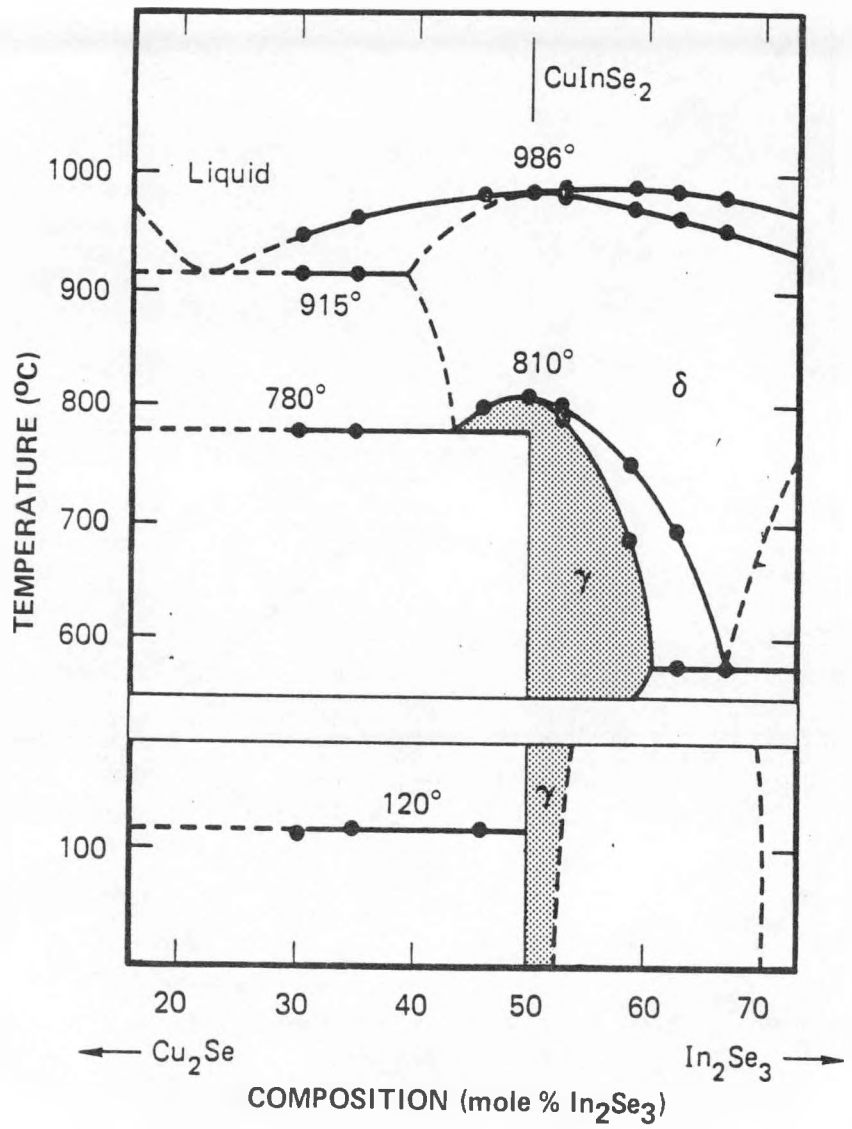

Fig. 7. Cu_2Se–In_2Se_3 pseudobinary phase diagram.

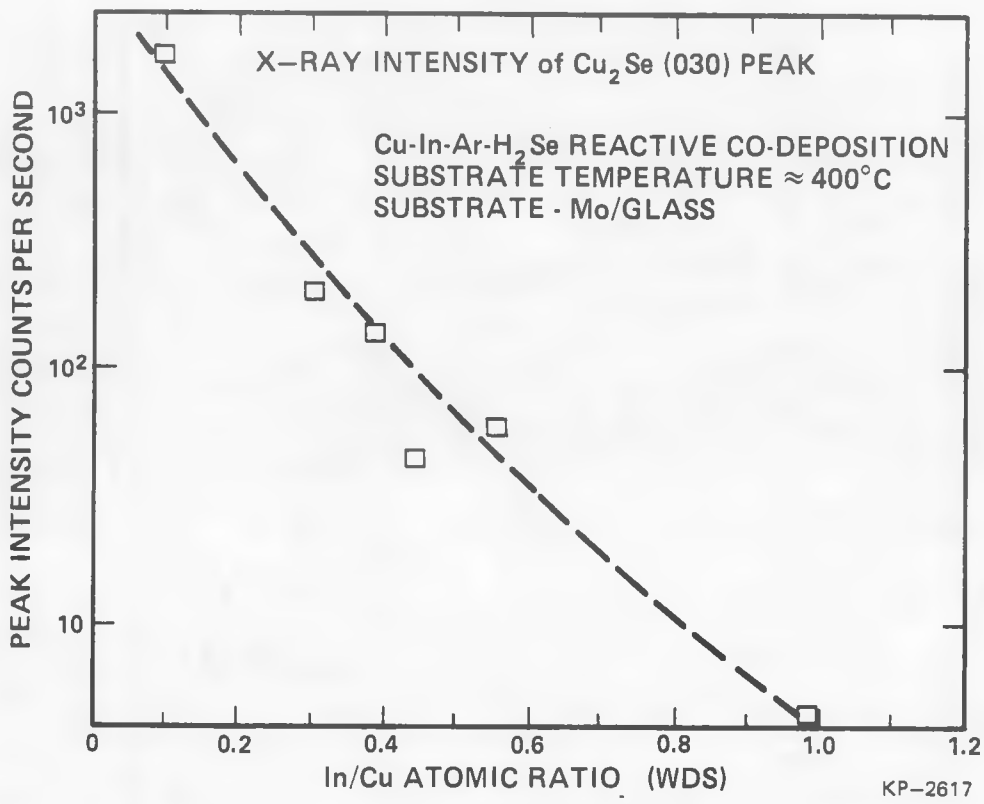

Fig. 8. Peak intensity of Cu_2Se 030 X-ray line as a function of the In/Cu concentration ratio for two-phase Cu_2Se-$CuInSe_2$ films on the Cu-rich side of the resistivity peak shown in Fig. 6.

rich side of the stoichiometric boundary has a single phase chalcopyrite structure. In all cases the $CuInSe_2$ phase exhibited a strong [112] preferred orientation, which was actually more pronounced for the Cu-rich films. The [112] orientation is the one which places the most densely packed Se plane adjacent to the substrate surface and is the expected orientation at substrate temperatures that are too low to cause recrystallization. Table 2 shows X-ray diffraction data for typical films from the Cu-rich side (Sample A) and the In-rich side (Sample B) of the stoichiometric composition, compared to the $CuInSe_2$ and Cu_2Se powder files. Sample A shows prominent $CuInSe_2$ and Cu_2Se_2. Sample B shows only the $CuInSe_2$ lines.

Figure 9 shows total transmission and total reflection data for four films marked by the symbol "x" in Fig. 6. The measurements were made with the UV/VIS/NIR spectrometer equipped with an integrating sphere which is described in Section 2. The spectra of the films from the In-rich single phase (samples 6153 and 6144) region show total absorption below the bandgap and virtually no absorption in the near-infared region. By contrast, the films from the Cu-rich two-phase region (samples 6168 and 6166) show relatively high absorption throughout the near infared. This is identical to the behavior reported by Megerle et al. for evaporated coatings. They also found absorption at wavelengths beyond the band edge for films containing the highly conductive Cu_2Se phase, and no absorption in this region for single phase films.

The composition and crystallographic variations discussed above also manifest themselves in the surface topography of the coatings. The photomicrographs in Fig. 10 show the surface topography of Cu-In-Se coatings having Cu-rich, stoichiometric and In-rich compositions. All the coatings were deposited onto glass substrates at 400°C, have the same nominal thickness (500 nm), and are shown at the same magnification (10,000X). The coatings which represent the three resistivity regions in Fig. 6 seem to have distinctly different structures. The Cu-rich film is characterized by surface features about 0.75 micron in size and isolated nodular surface growths. Microprobe analysis does not indicate a detectable difference in composition between the nodular surface growths and the background material. The In-rich film exhibits what appears to be a faceted sur-

TABLE 2
X-ray Diffraction Data Comparing Two Thin-Film Samples with Powder Files
{Sample A (Cu/In > 1) Sample B (Cu/In < 1)}

$CuInSe_2$ Powder File 23-209

d_{pow}	d_A	d_B	I/I_o (pow)	I/I_o (A)	I/I_o (B)	hkl
5.20		5.19	6		0.4	101
3.34	3.34	3.33	70	100	100	112
3.20		3.21	6		1	103
2.52	2.51		15	0.005		211
2.15		2.15	6		0.5	105,213
2.04	2.05	2.04	100	0.13	26	204,220
1.74	1.74		85	0.04		116,312
1.48		1.48	6		0.12	305,323
1.45	1.44	1.45	25	0.007	0.78	008,400
1.39		1.40	4		0.18	217,411
1.33	1.33	1.33	35	0.007	2.5	316,312

Cu_2Se Powder File 27-1131

d_{pow}	d_A	d_B	I/I_o (pow)	I/I_o (A)	I/I_o (B)	hkl
6.83	6.82	----	40	.71	----	030
2.27	2.26	----	40	0.08	----	090

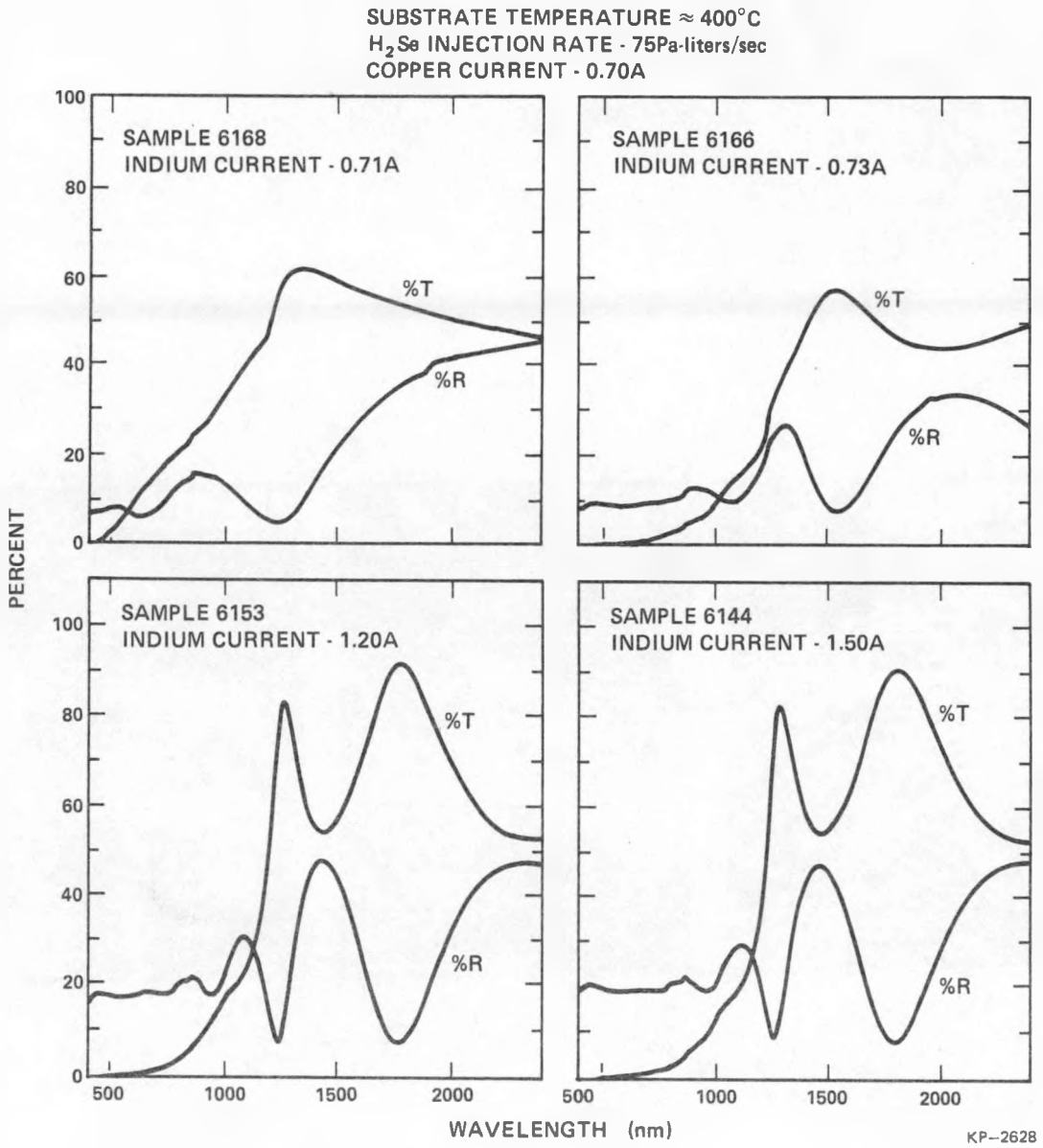

Fig. 9. Total transmission (%T) and total reflection (%R) data for films deposited at various currents to the In source with a fixed current of 0.7A to the Cu source, injection rate of 75 Pa-liters/sec and substrate temperature of 400°C. The four films are identified by the symbol "x" in Fig. 6.

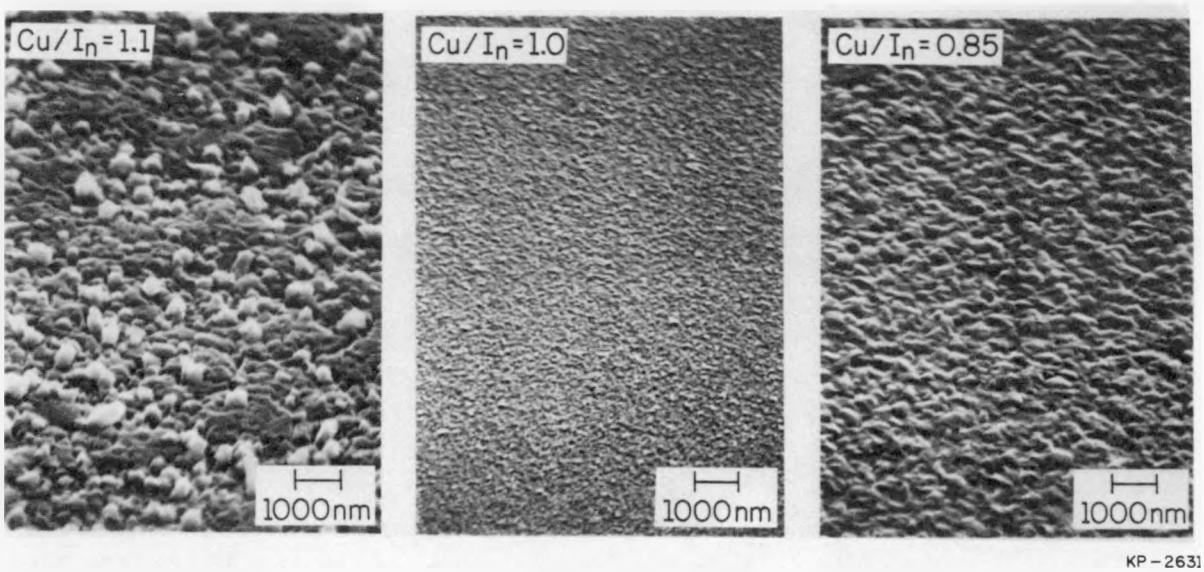

Fig. 10. SEM photomicrographs showing surface topography of Cu-In-Se coatings with Cu-rich, stoichiometric and In-rich compositions. Coating thickness ~ 500 nm.

face with features about 0.25 microns in size, consistent with the previous Telic work.[1] By contrast, the stoichiometric films are much smoother, with surface features in a range ($\sim$ 0.1 micron) that is difficult to resolve well with a scanning electron microscope.

The observations described above for the reactive sputtered coatings are generally consistent with those reported for evaporated coatings. Thus Noufi et al. have reported that their Cu-rich films contained $CuInSe_2$ and $Cu_{2-x}Se$ phases and that their In-rich material contained mixed phases and regions of sphalerite structure.[9] Megerle et al. have reported that their Cu-rich films contained tetragonal Cu_2Se, cubic $Cu_{2-x}Se$ ($x \approx 0.15$), and alpha cubic Cu_2Se, as well as $CuInSe_2$.[8] Their In-rich films contained hexagonal In_2Se_3 and other less common phases as well as $CuInSe_2$. Both Noufi et al. and Megerle et al., and also Stolt et al., have reported a single phase $CuInSe_2$ structure in the vicinity of the stoichiometric composition. However, in contrast to the phase diagram interpretation of the sputtering data suggested above, these investigators conclude that the single phase region in their evaporated coatings extends on both sides of the stoichiometric composition, with the medium resistivity material on the Cu-rich side being single phase p-type $CuInSe_2$. Megerle et al. report that their high resistivity n-type material contained In_2Se_3 as a second phase and that the low resistivity p-type material contained Cu_2Se as a second phase.

The relevant question is whether there are any fundamental differences between the reactive sputtered and the co-evaporated $CuInSe_2$ coatings. Phase diagrams are useful in sorting out the macroscopic metallurgical properties but do not speak to the issue of the electronic properties. These properties are determined by the defect structure of the lattice at a level that cannot, in general, be detected by concentration measurements. Therefore, as pointed out in the semiannual report,[7] a thin p-type $CuInSe_2$ region may well exist on the Cu-rich side of the resistivity peak shown in Fig. 6. The defect structure on $CuInSe_2$ is not well understood. Possible acceptors are Cu vacancies, In vacancies, Se interstitials, or Cu atoms on In sites. Possible donors are Se vacancies, In interstitials, Cu interstitials, or In atoms on Cu sites. Various investigators have shown that p-type conductivities on $CuInSe_2$ crystals are promoted by an excess of Se, while n-type behavior is

promoted by a deficiency of Se.[20,21] Thus careful attention to the Se content is important in comparing data. Fig. 11 shows the composition data in Fig. 6 plotted on a portion of the ternary phase diagram surrounding the stoichiometric composition. The data straddle the tie line on which the $Cu_2Se - In_2Se_3$ phase diagram is defined, suggesting that the reactively sputtered films do not have a intrinsic tendency toward a Se deficiency. The existence of a narrow single phase p-type chalcopyrite region on the Cu-rich side of the stoichiometric composition could be explained by Cu atoms on In sites. Similarly, the n-type conductivity in the single phase n-type chalcopyrite region of the sputtered coatings could be explained by In atoms in Cu sites. Future work should provide greater insights into this behavior. However, it is important to keep in mind that the evaporated $CuInSe_2$ films that have been found to be useful in fabricating the highest performance $CuInSe_2$/CdS cells are found to have compositions within the outlined region shown in Fig. 11 and to have n-type conductivities which are apparently type-converted during cell fabrication.

Finally a comment should be made regarding the dependence of the data shown in Fig. 6 on the In discharge current. The Cu-rich region formed at low In currents is characterized by relatively abrupt changes in both conductivity and film composition. By contrast, the In-rich region at higher discharge currents is characterized by much smaller changes in resistivity and composition; i.e., a factor of two change in current to the In source is seen to cause an increase in the In composition of only about 1 at %. These nonlinear dependences are due partly to the character of the $CuInSe_2$ material, as discussed previously, and partly to processing effects. There are two important processing effects. The first relates to variations of the In sticking coefficient with the composition of the deposition surface and the second relates to surface layer formation on the In sputtering target. The latter effect appears to have caused the actual flux of sputtered In atoms to vary nonlinearly with the current to the In source. These behaviors are discussed in the next section.

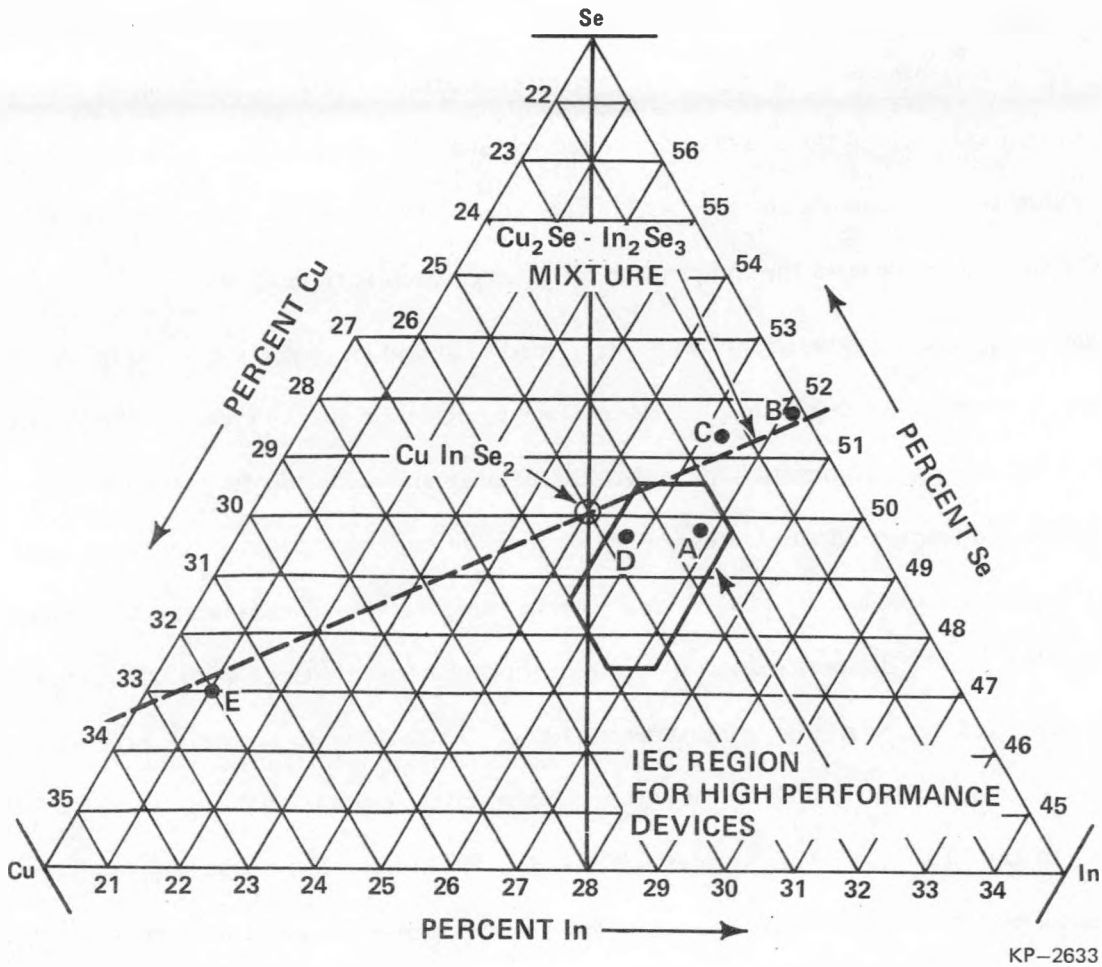

Fig. 11. Composition data from Fig. 6 plotted on ternary Cu-In-Se phase diagram covering the region surrounding the stoichiometric composition.

4.3. Deposition Flux and Sticking Coefficient Measurements

Evaporated $CuInSe_2$ coatings are generally grown with an excess flux of Se that is sufficient to produce Se saturated films. At elevated substrate temperatures excess Se, beyond that which can be accommodated into a coating by the incident metal atom flux, is rejected. Thus, the high-temperature Se sticking probability depends on the surface composition of the growing coating and under typical deposition conditions is considerably less than one. A similar approach is used in the reactive sputtering process, with H_2Se injection rates selected to provide Se fluxes at the substrate which considerably exceed the fluxes of sputtered metal atoms, as discussed in Section 4.1. A great deal of evidence also supports the proposition that at elevated substrate temperatures the In sticking coefficient is dependent on the composition of the deposition surface.

Reactive sputtering experiments were performed to obtain an indication of the In and Se sticking coefficients, and their dependence on the surface composition of the growing film for the same range of sputtering conditions that provided the data given in Fig. 6. In particular the coatings were deposited on unheated substrates ($\sim$ 30°C) that are expected to have condensed most of the arriving deposition species. Relative sticking coefficients were then estimated by comparing the fluxes implied by the deposition rate and composition of these coatings with the composition of coatings deposited under similar conditions at 400°C. Thus the cold substrate experiments were conducted with a current of 0.7A to the copper source and currents in the range from 0.3A to 1.5A delivered to the In source. The Ar pressure was 0.2 Pa and the H_2Se injection rate was 75 Pa-liters/sec. The deposition time in each experiment was 5 min. The substrate temperature did not exceed 30°C. The coating thicknesses were determined by a Tencor Instruments Alpha-Step Stylus instrument. They were in the range from 200 to 800 nm. The film compositions were determined by Auger electron spectroscopy, with the samples being Auger depth profiled by Ar bombardment to remove surface contamination and until the signals no longer changed. The Cu, In and Se compositions were deduced from the Auger elemental calibration factors with no corrections for matrix effects.

Figure 12 shows the elemental deposition fluxes implied by the coating thickness and composition data, as a function of the current to the In source. Three things are apparent.

- The Cu flux is seen to be constant, implying that the Cu sticking coefficient is also constant. We have no reason to believe, in fact, that the Cu sticking coefficient is not near unity.
- The In flux is seen to vary linearly with the current to the In source, but to be negligible for currents of less than 0.5A. It is difficult to imagine a mechanism that would vary the In sticking coefficient in a way that would produce this behavior, particularly since operating the In sputtering source by itself at a current of 0.25A did not produce a measurable deposition rate. The linear dependence suggests a constant sticking coefficient and we have no reason to expect that the In sticking coefficient was also not near unity in this region. We therefore believe that the explanation for the low In deposition at low currents lies in surface layer formation on the In target surface. At low sputtering rates a layer consisting primarily of Se-containing species may be maintained on the target surface by incident Se bearing gas species, so that the sputtered species are primarily atoms from this layer and not In.
- The Se incorporation appears to track the total metal (Cu and In) incorporation rate. This suggests that the Se sticking coefficient may be less than unity. We do not know the form of the Se reaching the substrate, although we expect no contribution from H_2Se in the gas phase. The Se flux probably arrives as SeII and Se species from the plasma and the sputtering target, but the experiment does not give information on the magnitude.

Figure 13 shows the relative In sticking coefficient as a function of coating composition for Cu-In-Se coatings deposited at about 400°C onto glass substrates, and at about 450°C on Mo coated glass substrates, using the same Cu and In discharge currents as were used in the data shown in Fig. 12. At each discharge current the In sticking coefficient was calculated from the flux data in Fig. 12 and the composition of the high temperature coating by assuming that the Cu sticking coefficient was identical in both cases. The assumption that the Cu sticking coefficient was not reduced at the elevated temperatures is based on the fact that identical sticking coefficients between the hot and cold cases are implied by those high temperature coatings for which we have both composition and deposition rate data. The assumption is also consistent with recent observations by Stolt et al.[10] In particular, Stolt et al. deposited Cu—In—Se_2 films by co-evaporation from Cu, In and Se sources with a mass spectrometer arranged to monitor the arrival fluxes. Films deposited with fixed fluxes of Cu and In and a variable flux of Se yielded a variable In/Cu ratio but all contained the same amount of Cu atoms. Similarly, films deposited with fixed fluxes of Cu and Se and a variable flux of In yielded a variable In/Cu ratio, but again the number of Cu atoms in all the films was found to be constant.

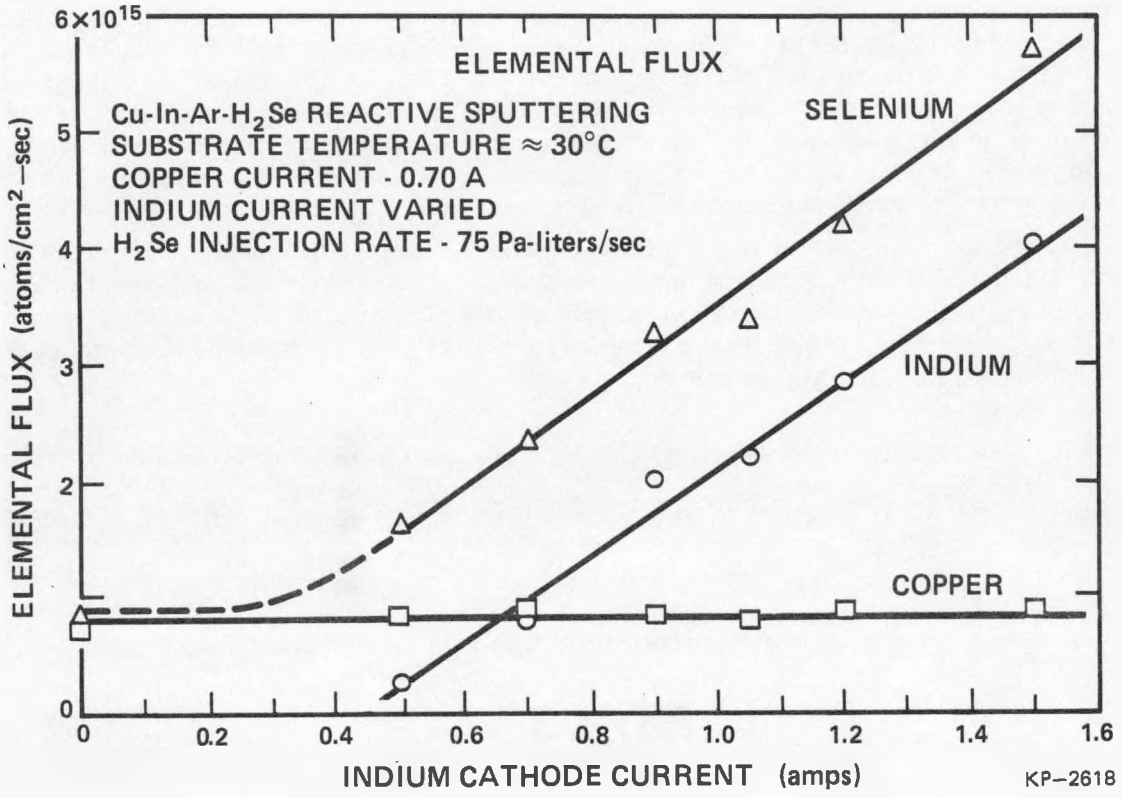

Fig. 12. Copper, indium and selenium elemental substrate fluxes implied by composition and deposition rate measurements on reactive sputtered Cu-In-Se coatings deposited at various currents to the In source with a fixed current of 0.7A to the Cu source, injection rate of 75 Pa-liters/sec and substrate temperature of 30°C.

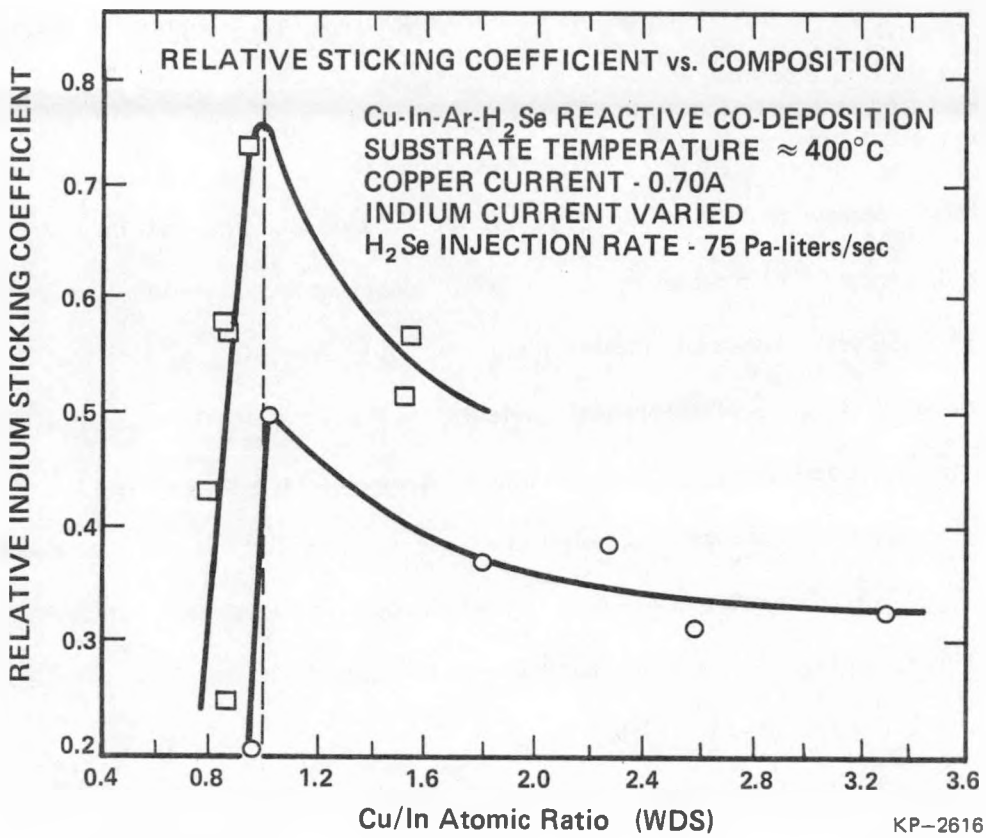

Fig. 13. Relative sticking coefficient of sputtered In flux as a function of coating composition for Cu-In-Se coatings deposited on glass substrates at about 400°C and on Mo coated glass substrates at about 450°C. Relative sticking coeffiicent is defined as the ratio of the implied sticking coefficient at the stated deposition temperature divided by the sticking coefficient implied by deposition rate and composition measurements made on coatings deposited on a 30°C substrates.

Referring to Fig. 13, the relative In sticking coefficient is seen to be maximum for a stoichiometric film and to decrease for off-stoichiometric films that are rich in either Cu or In. The reduced sticking coefficient on the Mo coated substrate is thought to be simply a matter of the higher substrate temperature which developed due to the lower emittance of the Mo coated substrate.[22] Relative sticking coefficients between the cold and hot substrates were also estimated for Se. The data exhibits a functional dependence on composition that is similar to that of In, but are not shown in the figure because of our lack of knowledge concerning the Se flux and the role H_2Se reactions on the hot substrate surface.

The rapid decrease in In sticking coefficient for the In-rich films may be a consequence of a reduced binding energy for In atoms in those types of sites that would yield an In-rich chalcopyrite material, i.e., In interstitials and In atoms on Cu sites. It is interesting to note that Zunger et al.[23] have concluded on the basis of theoretical modeling that, even at the In chalcopyrite sites, the In bonding to the surrounding Se atoms is considerably weaker than that of the Cu atoms at their respective sites. The fact that we were able to produce n-type $CuInSe_2$ films with a small excess of In (2%, see Fig. 6), by depositing at elevated temperatures with a large excess in the incident In flux (factor of 3 to 5, see Fig. 12), suggests that the n-type conductivity might indeed be attributed to In atoms at Cu sites or at interstitial sites.

5. DEVICE FABRICATION

5.1. Two Layer $CuInSe_2$ Deposition Experiments

As discussed in Section 4.2, the range of deposition conditions that yield the desired p-type single phase chalcopyrite material for device fabrication is very narrow. The situation is complicated by significant variations in the sticking coefficients in the immediate vicinity of the stoichiometric composition, which make the composition of the film not proportional to the composition of the arrival flux (see Section 4.3 and Ref 10). This has led to wide use of the two-layer approach developed by Boeing, which appears to widen the "deposition window". In this approach photovoltaic $CuInSe_2$ coatings are formed as a two layer composite of the material deposited on each side of the resistivity peak shown in Fig. 6. Typical composition of the base-layer, top-layer and of the final composite coating, as measured by X-ray fluorescence, is given below.[13]

First Layer - 2700 nm (At. %)			Second Layer - 1300 nm (At. %)			Composite Layer Measured (At. %)			Composite Layer Calculated (At. %)		
Cu	In	Se	Cu	In	Se	Cu	In	Se	Cu	In	Se
26.2	25.7	48.1	20.0	30.7	50.3	24.4	26.7	48.2	24.5	27.4	48.8

The base-layer is typically deposited at 350°C and is p-type. The top-layer is typically deposited at 450°C and if isolated would be n-type. Interdiffusion during the deposition appears to cause considerable intermixing, so that the final composition is approximately that which one would calculate from the total atomic composition of the two sub-layers, as shown by the calculated values in the table. There is, however, some evidence of a slight compositional gradient in the composite coatings with the surface being rich in In.[24] The n-type In-rich composite coating is apparently type-converted during the cell fabrication process. The range of composite layer compositions which have been found to yield high performance devices at the University of Delaware Institute of Energy Conversion is

Cu = 23.0 to 26.0% In = 25.4 to 27.2% Se = 47.4 to 50.7%

This range is identified in the ternary phase diagram shown in Fig. 11.

An obvious question is whether the base-layer and top-layer compositions listed above are unique, or whether other "building block" compositions could be used, provided the layer thickness were selected to place the mixed composition within the window for high performance material. We have investigated this issue by depositing composite coatings in which the base layers were made much richer in Cu and the top layers were made more nearly stoichiometric, as shown by the following table.

Base Layer (At. %)			Top Layer (At. %)		
Cu	In	Se	Cu	In	Se
32.0	21.0	47.0	23.0	27.0	50.0

Table 3 shows composition data for a series of composite films formed from these building blocks with base layers of varied thicknesses and fixed top layer thicknesses. The compositions measured at IEC using energy dispersive X-ray fluorescence show clear evidence of mixing, but are not in particularly good agreement with the total mixing calculation. The one measurement which was made at SERI using wavelength dispersive X-ray fluorescence yielded excellent agreement with the total mixing calculation. The disagreement may be due in part to lateral gradients in coating composition, which were undoubtedly present since these coatings were deposited before the deposition shields discussed in Section 3, were installed. The IEC measurements were made at a fixed position on each sample, while the SERI data is an average taken over essentially the entire width of the sample. The composite coating listed in Table 3 were all Cu-rich and p-type. However, data certainly indicate that coatings within the desired composition range for high performance devices can be deposited from the base and top layers described above.

Two experiments were performed to explore the effect of the In sticking coefficient on the composition of the composite layer. In the first case the deposition temperature for the second layer was raised from about 400°C to about 450°C. This was expected to reduce the In sticking coefficient. Composition data are shown in Table 4 (sample 6201). The In composition was reduced slightly.

TABLE 3
Two-Layer Composited Coatings of Reactive Sputtered $CuInSe_2$

Sample Number	Bottom Layer* Deposition Time (Estimated Thickness)	Top Layer** Deposition Time (Estimated Thickness)	Calculated Composite Composition	Measured Composition IEC	Measured Composition SERI	Conductivity Type
6199	6 min (0.32 μm)	38 min (2.55 μm)	Cu=24.05 In=26.28 Se=49.65	Cu=26.1 In=25.5 Se=48.4	--	p-type
6195	9 min (0.48 μm)	38 min (2.55 μm)	Cu=24.53 In=25.98 Se=49.49	Cu=27.4 In=24.7 Se=45.9	--	p-type
6196	12 min (0.64 μm)	38 min (2.55 μm)	Cu=25.69 In=25.97 Se=48.33	Cu=29.5 In=24.6 Se=45.9	--	p-type
6197	15 min (0.78 μm)	38 min (2.55 μm)	Cu=25.02 In=25.06 Se=49.27	Cu=26.3 In=25.7 Se=48.0	--	p-type
6198	18 min (0.96 μm)	38 min (2.55 μm)	Cu=25.52 In=25.34 Se=49.65	Cu=30.3 In=23.9 Se=48.4	Cu=25.67 In=24.44 Se=49.90	p-type

* Cu = 32.0%, In = 21.0%, Se = 47.0%, Dep. Rate = 53 nm/min

** Cu = 23.0%, In = 27.0%, Se = 50.0%, Dep. Rate = 67 nm/min

TABLE 4
Two-Layer Reactived Sputtered $CuInSe_2$

Sample Number	Bottom Layer* Deposition Time (Estimated Thickness)	Top Layer Deposition Time (Estimated Thickness)	Measured Composition IEC	Measured Composition SERI	Conductivity Type
6201	18 min (0.96 μm) T = 350°C	38 min (2.55 μm) T = 450°C	Cu=31.1 In=23.0 Se=45.9	Cu=29.62 In=21.54 Se=48.85	p-type
6202	18 min (0.96 μm)	38 min (2.85 μm) I = 1.6A	Cu=24.4 In=26.3 Se=49.3	Cu=23.90 In=25.42 Se=50.68	p-type

*
Cu = 32.00%
In = 21.09%
Se = 49.85%
Dep. Rate = 53 nm/min

The second experiment was based on the premise that if rapid mixing were to occur during deposition, then the surface of the growing coating on top of the Cu-rich/base layer would remain richer in Cu than it otherwise would. Consequently, referring to Fig. 13, we would expect that the In sticking coefficient would be larger at any point during the film growth than it otherwise would and that the resultant composite coating would contain more In for a given second layer thickness than in a slow mixing case. Computer calculations which assume total mixing of the depositing material and In sticking coefficients that vary with surface composition, as shown in Fig. 13, are shown in Fig. 14 for two Cu-rich base layer compositions and three different In components in the deposition flux.

Figure 14a corresponds to deposition conditions similar to those used in Table 3, except that the In flux has been increased from 2×10^{15} atoms/cm^2-sec to 4.39×10^{15} atoms/cm^2-sec (discharge current from 1 to 1.6A). The rapid accumulation of In in the *in situ* mixing case is clearly apparent, with top layer thicknesses of only about one-fifth the bottom layer thickness being required to achieve stoichiometric composition of the composite. Post-deposition mixing corresponds to the extreme of the slow mixing case, where the composition of the two layers prior to mixing is the same as if the two layers were deposited independently on glass substrates. Sample 6202 in Table 3 was deposited under the conditions shown in Fig. 14a. Composition data obtained by X-ray fluorescence at SERI and IEC are given in Table 3 and plotted in Fig. 14a. The experimental data (shown by the open and solid circles) is in excellent agreement with the post-deposition mixing calculation.

Figure 14b corresponds reasonably closely to base layer and top layer compositions for a typical Boeing type composite layer. In these coatings the second layer is made about one-half the thickness of the base layer. Experimental composition measurements for the composition of a Boeing top layer[13] are shown by the solid circle data point in the figure. Again the agreement is excellent, when one takes into account that the computer calculation was made using a top layer In composition that was about 10% lower than that used in the Boeing work.

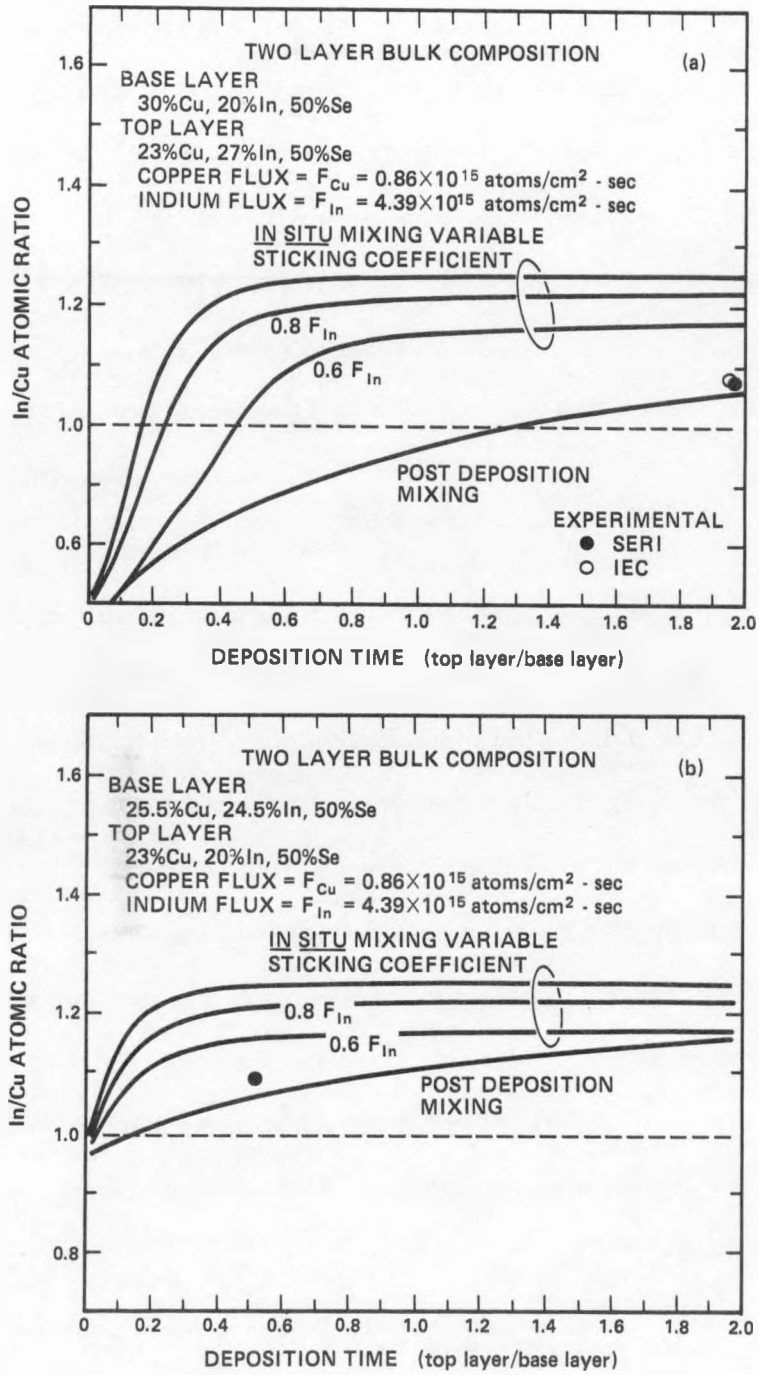

Fig. 14. Computer calculations for In/Cu ratio in Cu-In-Se coatings as a function of top layer thickness, for indicated base layer compositions and various In/Cu ratios in the deposition flux. The calculations assume total instantaneous compositional mixing and that the In sticking coefficients obey the functional dependence shown in Fig. 13. Calculations are also shown for the case where no mixing occurs until the top-layer deposition is complete.

Thus the evidence suggests that the mixing is almost complete but does not occur fast enough to influence the deposition process itself. Devices of reasonable efficiency ($\sim$ 5%) have been fabricated from composite material of the type represented by sample 6202 in Table 3 and data points in Fig. 14a. Thus it appears that one can indeed fabricate reasonable devices from composite $CuInSe_2$ layers built from base and top layers that are very different in composition from those used by most groups. However, more efficient cells would be required to provide a definitive answer to this question.

5.2. Device Fabrication at IEC

$CuInSe_2$/CdS devices were fabricated at IEC from reactive sputtered $CuInSe_2$ which was deposited onto Mo-coated glass and alumina substrates at Illinois. The procedure is described in detail in Ref. 1. The cell configuration is shown in Fig. 15. The IEC cell fabrication process consists of (1) evaporating CdS (usually with In doping) onto the CuInSe, (2) sputtering a tin-doped indium oxide (ITO) top electrode/AR layer onto the CdS, (3) depositing a pattern of Ni contacting bus bars onto the CdS and (4) using photolithographic methods to etch the ITO and CdS and thereby form an array of twelve 3 mm × 3 mm photovoltaic cells over the 24 mm × 24 mm substrates as shown in Fig. 15. Following fabrication, the cells were heat-treated in air at 200°C to optimize their performance.

As cited previously, The experience at IEC has been that devices with efficiencies of greater than 9% have two-layer composite $CuInSe_2$ coatings with X-ray fluorescence compositions in the range Cu = 24.5 ± 1.5%, In = 26.3 ± 0.9%, and Se = 49.2 ± 1.5%. This range of composition is shown by the outlined region in Fig. 11, and was used as a guide determining whether particular coatings should be processed into cells. Table 5 summarizes the $CuInSe_2$ layer composition measurements and the data for the best cell on each substrate that was processed.

The first cell fabrications were made using single layer $CuInSe_2$ coatings, about 2500 nm thick, deposited onto unpolished alumina substrates with a Mo base electrode. Although the compositions of several of these coatings were within the desired IEC composition range, none yielded

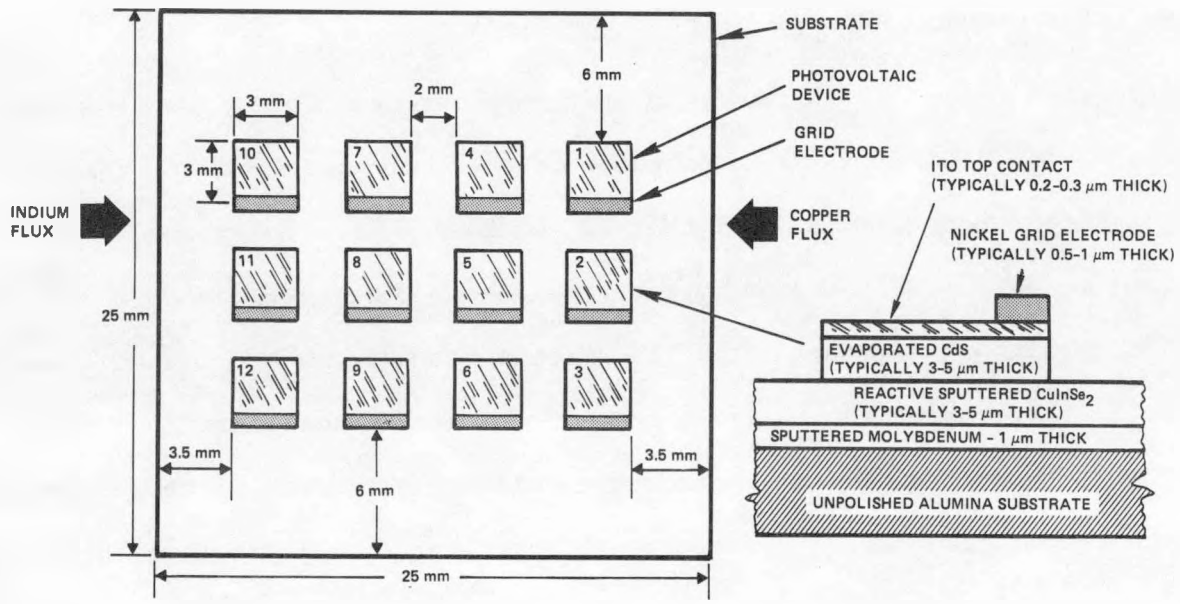

Fig. 15. General configuration of $CuInSe_2/CdS$ cells which were fabricated at IEC to evaluate the reactive sputtered $CuInSe_2$.

TABLE 5
Coating Composition and Cell Performance Data

Sample Number	Coating Configuration	Composition, Atomic Percent* Cu	In	Se	Cell Performance J_{Sc} (mA/cm²)**	V_{oc} (V)	FF (%)	η (%)
6048C	S/A	+ 24.2 22.4†	26.9 26.2†	48.9 51.3†	~ 30	⩽ 0.1	--	--
6053C	S/A	25.1	27.5	47.4		Shorted		
6176	D/G	25.1	23.8	51.0	24.82	0.192	40.23	1.92
6179	D/G	26.0	24.8	49.2	34.12	0.176	41.72	2.50
6180	D/G	28.8	23.7	47.5	18.75	0.146	30.08	0.79
6181	D/G	24.3	25.2	50.4	25.01	0.196	31.75	1.55
6182	D/G	+ 25.9	25.4	48.7	31.46	0.231	43.35	3.15
6183	D/G	27.9	23.8	48.3	12.89	0.017	25.0	--
6184	D/G	28.9	23.7	47.4	33.39	0.1612	37.41	2.01
6188	D/G	23.6	24.7	51.9	28.86	0.208	48.65	2.85
6197	D/G	26.3	25.7	48.0	26.85	0.154	31.47	1.30
6199	D/G	26.1	25.5	48.4	23.44	0.212	35.57	1.76
6202	D/G	+ 24.4	26.3	49.3	24.75	0.373	60.06	5.51
6204	D/G	+ 25.8	25.9	48.3	14.80	0.061	27.64	0.25
6223	D/G	+ 25.9	25.8	48.3	31.64	0.319	50.86	4.86
6233	D/G	+ 25.5	26.5	48.0	17.94	0.10	28.9	0.5

* Measured by energy dispersive X-ray fluorescence at IEC.

** Based on light intensity of 100 mA/cm².

† Measured by wavelength dispersive X-ray fluorescence at SERI.

\+ Compositions in the IEC range for best cell performance. see Fig. 11.

good devices. Examples are cells 6048C and 6053C in Table 5.

Our first series of composite two-layer $CuInSe_2$ coatings were deposited by combining a 1750 nm thick In-rich top layer, having a nominal composition of Cu = 23.5%, In = 26.5%, Se=50%, with 3250 nm thick Cu-rich base layers deposited with sputtering currents selected to give compositions in the range from Cu = 30%, In = 20%, Se = 50% to Cu = 25%, In = 25%, Se = 50%. Both layers were deposited at a nominal temperature of 400°C on Mo-coated glass substrates. Although all but one of the cells in this series was rich in copper and outside of the preferred range for device applications, all of the samples (6176 through 6188 in Table 4) were fabricated into cells. The one coating that was within the preferred range (#6182) yielded a device with an efficiency of 3.15%.

Two problems were recognized during the deposition of the composite two-layer coatings described above. First, the composition of the coatings did not scale as faithfully as expected with the In/Cu current ratios used in the deposition of the Cu-rich base layers. This is believed to have been a consequence of the extremely strong dependence of the coating composition on the Cu/In current ratio, as shown in Fig. 6. As discussed in Section 4.3, subsequent experiments have shown that this behavior is due in part to surface layer formation on the In sputtering source at low discharge currents and is not believed to be a fundamental problem. Second, the coatings exhibited composition gradients because of the geometric locations of the sputtering sources as described in Section 3. The composition dependence of the In sticking coefficient (see Fig. 13) tends to make the In-rich top layer films have a spatially uniform composition, since reactions at the surface reject excess In and thereby promote the formation of a nearly stoichiometric deposit even when the arriving fluxes are not of uniform composition (see Ref. 7, p. 26). However, this type of reaction does not intercede for the Cu-rich base-layer films. Consequently concentration gradients were found in the two-layer composite films, particular when excess Cu was present.

Because of the difficulty that was experienced in controlling the base layer composition in the composite two-layer films described above, it was not possible to draw definite conclusions regarding the contributions of the base and top layers to the composition of the composite film. Therefore

the series of composite two-layer films described in Section 5.1 and listed in Table 3 were deposited. In these films the Cu content was controlled by controlling the thickness of a Cu-rich base layer. Two of these films (#6197 and #6199) were within the preferred composition range and were fabricated into devices. They yielded efficiencies of about 1.5%. Sample 6202 was fabricated in a subsequent experiment in which a larger In flux was used during the deposition of the top layer (see Section 5.1). This film was also within the preferred composition range and yielded a device efficiency of 5.51%.

Following the fabrication of the 5.51% cell, a series of deposition runs were made to examine the consistency of the reactive sputtering process by attempting to duplicate composite films of the same type that had yielded the reasonable performance. The results of these deposition runs are shown in Table 6, where the data identified with an "A" are average values for three substrates coated during the run. The compositions of all the samples were within the preferred range for device fabrication, and the run-to-run consistency was excellent. Thus the standard deviation, expressed as a percent of the average value, was in the range of 1 to 3%. Thus there seems to be little question regarding the reproducibility of the sputtering process. However, cell fabrication yielded only one device in this group with reasonable efficiency (#6223, η = 4.85%). The other devices were shorted. SEM examination indicated that the problem was a very rough surface topography on the $CuInSe_2$ coatings. The origin of the problem is believed to be the Cu-rich base layer which serves as a substrate for all subsequent depositions. As shown in Fig. 10, coatings with a high Cu content tend to have a rough surface topography. Thus we conclude that coatings within the composition range desired for device fabrication can indeed be formed using base layers with a higher Cu content (Cu = 32%, In = 21%, Se = 47%) than is normally used (Cu = 26%, In = 25%, Se = 49%), but that these high Cu content base layers have the disadvantage of a rough surface topography which influences the structure of all subsequent layers. Accordingly we will use a more conventional base layer composition in our future work.

TABLE 6
Consistency of Composition for $CuInSe_2$ Coatings
Deposited under Fixed Reactive Sputtering Condition

Sample Number	Bottom Layer Deposition Time (Estimated Thickness)	Top Layer Deposition Time (Estimated Thickness)	Composition (Atomic Percent) Cu	In	Se
6202	18 min (0.96 μm)	38 min (2.85 μm)	24.4	26.3	49.3
6204	18 min (0.96 μm)	38 min (2.85 μm)	25.8	25.9	48.3
6223	18 min (0.96 μm)	38 min (2.85 μm)	25.9	25.8	48.3
6224	9 min (0.48 μm)	19 min (1.43 μm)	25.8	25.8	48.4
6227 A	9 min (0.48 μm)	19 min (1.43 μm)	25.4	26.6	50.0
6228 A	9 min (0.48 μm)	19 min (1.43 μm)	25.1	25.9	48.9
6233 A	15 min (0.80 μm)	32 min (2.40 μm)	26.0	26.3	47.6
6234 A	12 min (0.64 μm)	24 min (1.80 μm)	25.0	26.0	48.9
6235 A	7 min (0.37 μm)	19 min (1.43 μm)	24.3	26.3	49.4
		Average	25.22	26.12	48.56
		Standard deviation	0.65(2.6%)	0.27(1.0%)	0.61(1.3%)
		IEC Range	23.0-26.0	25.4-27.2	47.4-50.7

A second observation relates to the composition variations across the substrate surface. These variations were such that in all cases distinctly higher performance was always seen for one row of three devices in the array shown in Fig. 15. Thus is was concluded that future device fabrication work would be delayed until the shields discussed in Section 3 and shown in Fig. 2 were installed.

A third observation relates to substrate temperatures. The general procedure when depositing composite two-layer $CuInSe_2$ coatings by co-evaporation is to use a substrate temperature of about 350°C when depositing the base layer and a temperature of about 450°C when depositng the top layer. The reactive sputtered coatings described above were deposited at a substrate temperature of about 400°C for both the base and top layers. Fig. 16 shows composition versus substrate temperature data for reactive sputtered Cu-In-Se coatings deposited with an excess flux of In during the Telic work.[4] The data suggest that the In sticking coefficient is near unity at low substrate temperatures, but that at temperatures in the range from 250 to 350°C excess In is rejected so that at temperatures in excess of about 350°C only a near stoichiometric $CuInSe_2$ material is deposited. Thus, beyond a substrate temperature of about 350°C, no major changes in composition are expected with substrate temperature. Several observations, including the sticking coefficient data shown in Fig. 13, suggest that our deposition at an indicated temperature of 400°C is in a range where clear substrate temperature effects are still discernible. Therefore, the use of higher substrate temperatures will be explored in our future work.

The compositions of $CuInSe_2$ coatings which yielded cells with efficiencies greater than about 1.5% are shown on the ternary phase diagram in Fig. 17. Because of the high absorption coefficient of $CuInSe_2$, relatively high currents can be generated, and efficiencies in the 2% range can be achieved in devices that are very far from the optimum for good efficiency. Thus efficiencies in this range are achieved for film composition outside the IEC range for good device performance. By contrast, every non-shorted cell within the IEC envelope yielded an efficiency in the 3 to 6% range. Therefore we see no reason why the consistent deposition of reactive-sputtered material which is within the preferred composition region and possesses a smooth surface topography will not permit

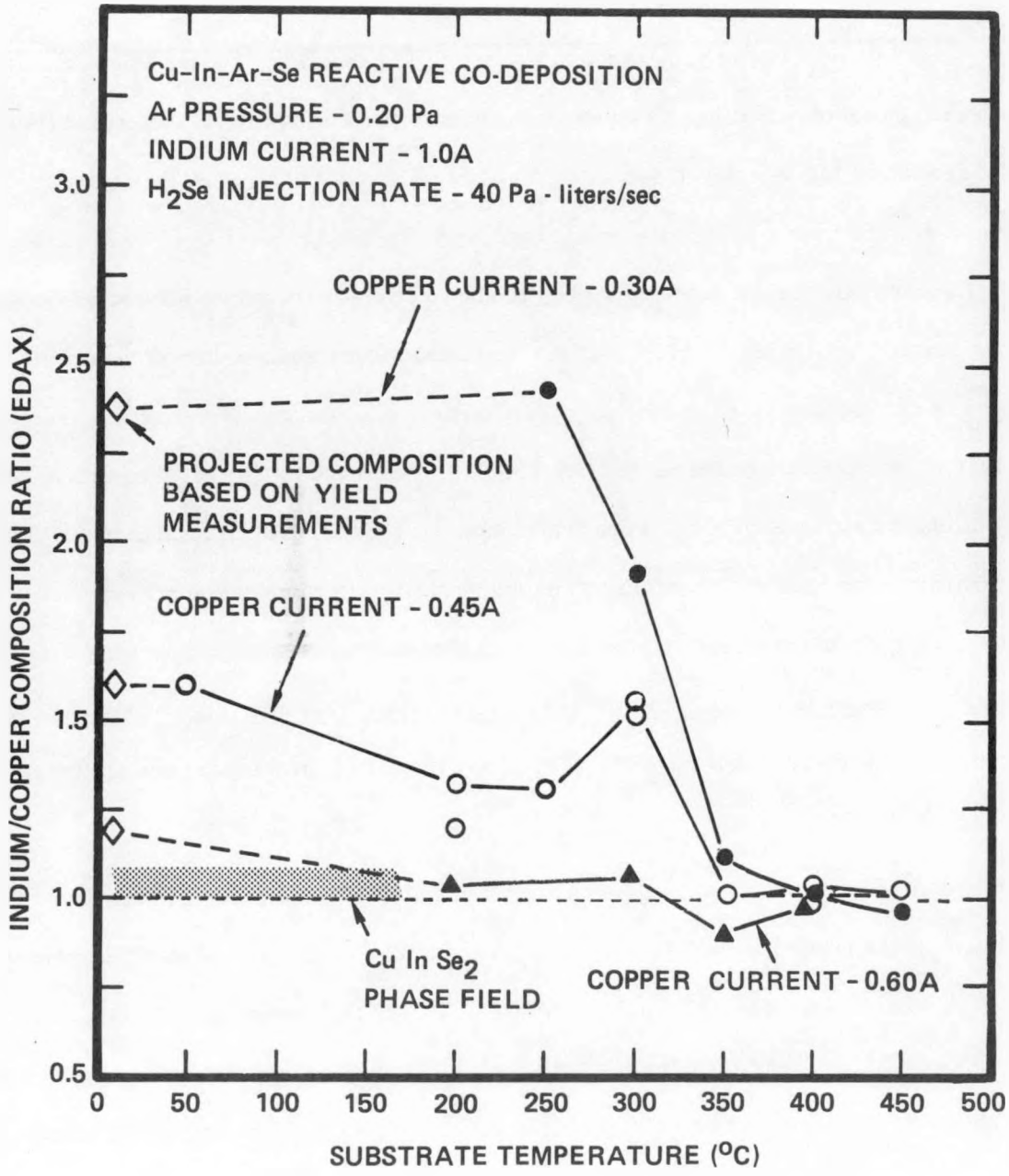

Fig. 16. In/Cu composition ratio versus substrate temperature for various currents to Cu source with a fixed current to In source. From Ref. 4.

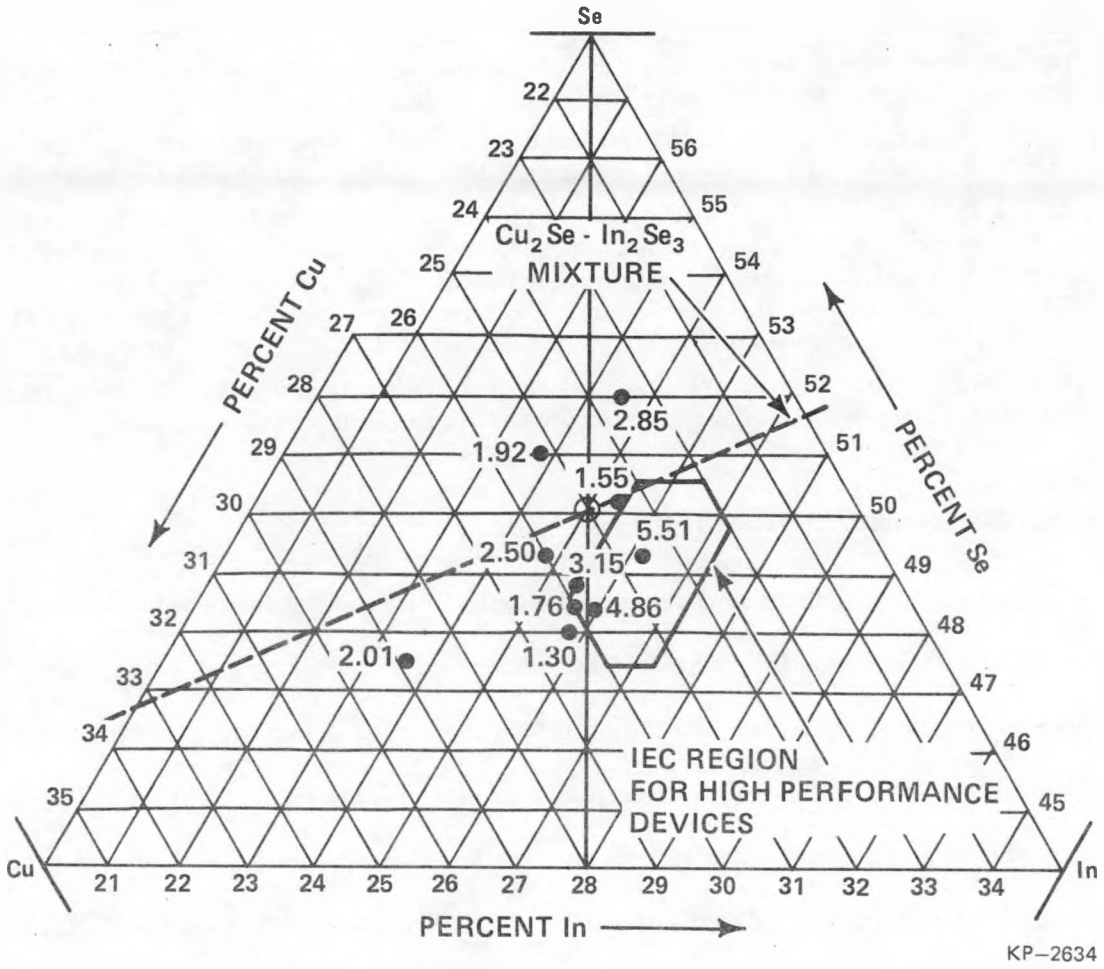

Fig. 17. Ternary Cu-In-Se phase diagram showing composition data for films that yielded $CuInSe_2/CdS$ devices with measurable efficiencies.

device optimization and the achievement of efficiencies comparable to those obtained with co-evaporated devices. The major emphasis in our future work will be toward this objective.

In summary, the following actions are being taken as a consequence of the observations described above.

- Deposition shields have been installed at the Cu and In sputtering sources to provide a more uniform Cu/In composition profile at the substrates. See Section 2 and Figs. 3 and 4.
- Quartz crystal rate monitors have been installed which will permit *in situ* measurements of the sputtering rates from the Cu and In sources. See Fig. 3.
- A Molytek Model 3702 datalogger has been installed in the system to monitor up to thirty-two process parameters. The system is initially being set up to monitor the current and voltage to each sputtering source, the substrate temperature and the substrate heater current, and voltage, and the Ar and H_2Se flow rates. The data logger accepts analog signals, plots and processes them, and delivers digital output data to an IBM PC for further processing.
- Composite two-layer $CuInSe_2$ coatings will be deposited using Cu-rich base layers that incorporate only a light excess in Cu and therefore that have a smoother surface topography.

5.3. Device Fabrication Activities at Illinois

An important aspect of the project is to develop a $CuInSe_2$/CdS device fabrication capability at Illinois. The CdS layers will be deposited by both reactive sputtering and evaporation. The in-line apparatus shown in Fig. 1 has two chambers dedicated to CdS deposition by reactive sputtering, so that all-sputtered $CuInSe_2$/CdS heterojunctions can be fabricated without breaking vacuum. Two chambers were allocated to this task in anticipation of depositing two-layer coatings such as undoped and In-doped CdS or (Cd,Zn)S and In-doped Cd. Thus a 99.9999% Cd target and a Cd target doped with 2 at. % In are presently installed in the in-line apparatus. Figure 18 shows a plain view of the CdS deposition stations. Initial shakedown work on the CdS reactive sputtering systems has been completed.

Figure 19 shows a schematic drawing of the chamber which has been configured for evaporating CdS semiconductor layers and Al grid electrodes. Thus evaporation sources for CdS and In are mounted on one side of the chamber, and a frame for mounting a resistive heated metal foil boat for evaporating the Al is arranged on the other side. The CdS and In evaporation sources are of the same type that are used at the University of Delaware Institute of Energy Conversion and were

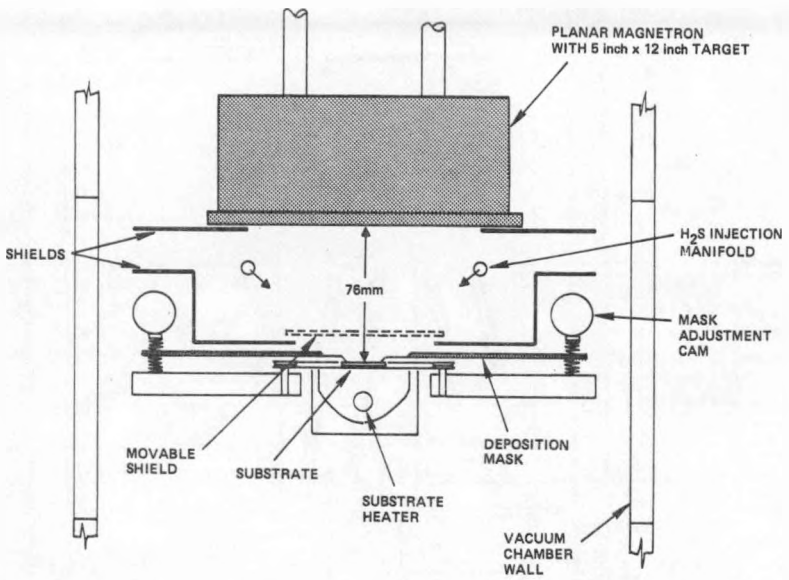

Fig. 18. Plan view illustration of CdS deposition chamber in the in-line sputtering apparatus.

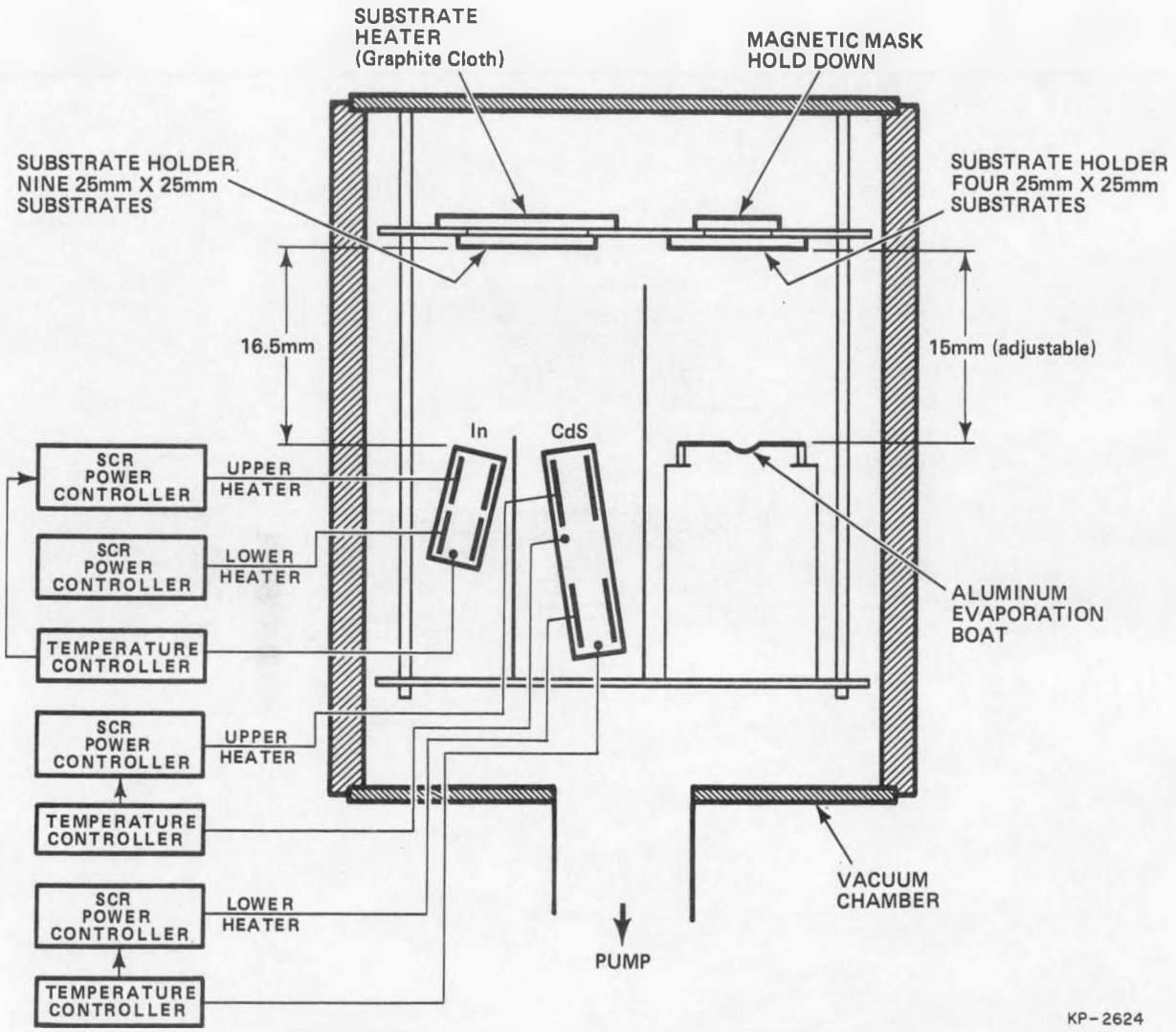

Fig. 19 Schematic drawing of evaporation chamber which has been assembled for CdS and Al evaporation.

manufactured at IEC. The sources use two heaters capable of independent control. In the CdS case, both heaters are independently controlled via Euratherm type 93/SCR power controllers which are driven by a Euratherm type 984 temperature controller using the outputs from thermocouples located in the upper and lower sections of the source. In the indium case the upper heater is set at a constant power, and the lower heater is controlled from a thermocouple located in the bottom of the source. Substrate heating for the CdS deposition is provided by resistive heating using graphite cloth. The system can accommodate nine 25 mm x 25 mm substrates. However, one substrate position is used to mount a Corning 7059 glass substrate with an imbedded chromel-alumel thermocouple for measuring the substrate temperature. Testing of the CdS evaporation sources is underway. The Al deposition system is configured to mount four 25 mm x 25 mm substrates. The grid electrodes are deposited using Kovar shadow masks which are held in place magnetically using small permanent magnets. Good line definition has been demonstrated for the evaporated Al grids.

It is anticipated that two cell configurations will be used. The initial configuration will consist of an array of twelve 3 mm x 3 mm cells on each 25 mm x 25 mm substrate, fabricated by procedures similar to those used at IEC and discussed in Section 5.2. Once devices with reasonable efficiency are being fabricated on a regular basis, we will begin using a 1 cm x 1 cm cell configuration. One difference between the cell fabricated at Illinois and those fabricated at IEC is that an aluminum grid rather than indium-tin-oxide with a Ni bus bar will be used as the top electrode. Figure 20 shows the electrode configuration that will be used for the 3 mm x 3 mm cells. The grid pattern will shadow about 17% of the cell but should be adequate for assessing the photovoltaic quality of various sputtered layers. Figure 21 shows the electrode configuration that will be used for the 1 cm x 1 cm cells. In this case the grid shadowing will be in the 5% range. Kovar deposition masks for both electrode configurations have been fabricated at Towne Laboratories and successfully tested in the Al evaporation chamber described above. The cell fabrication will therefore consist of depositing CdS over the entire $CuInSe_2$ substrate, using either reactive sputtering or evaporation. The Al top grid electrodes will then be deposited. Photolithography methods will then be used to define the solar cells by etching the CdS and $CuInSe_2$ layers. Antireflecting layers

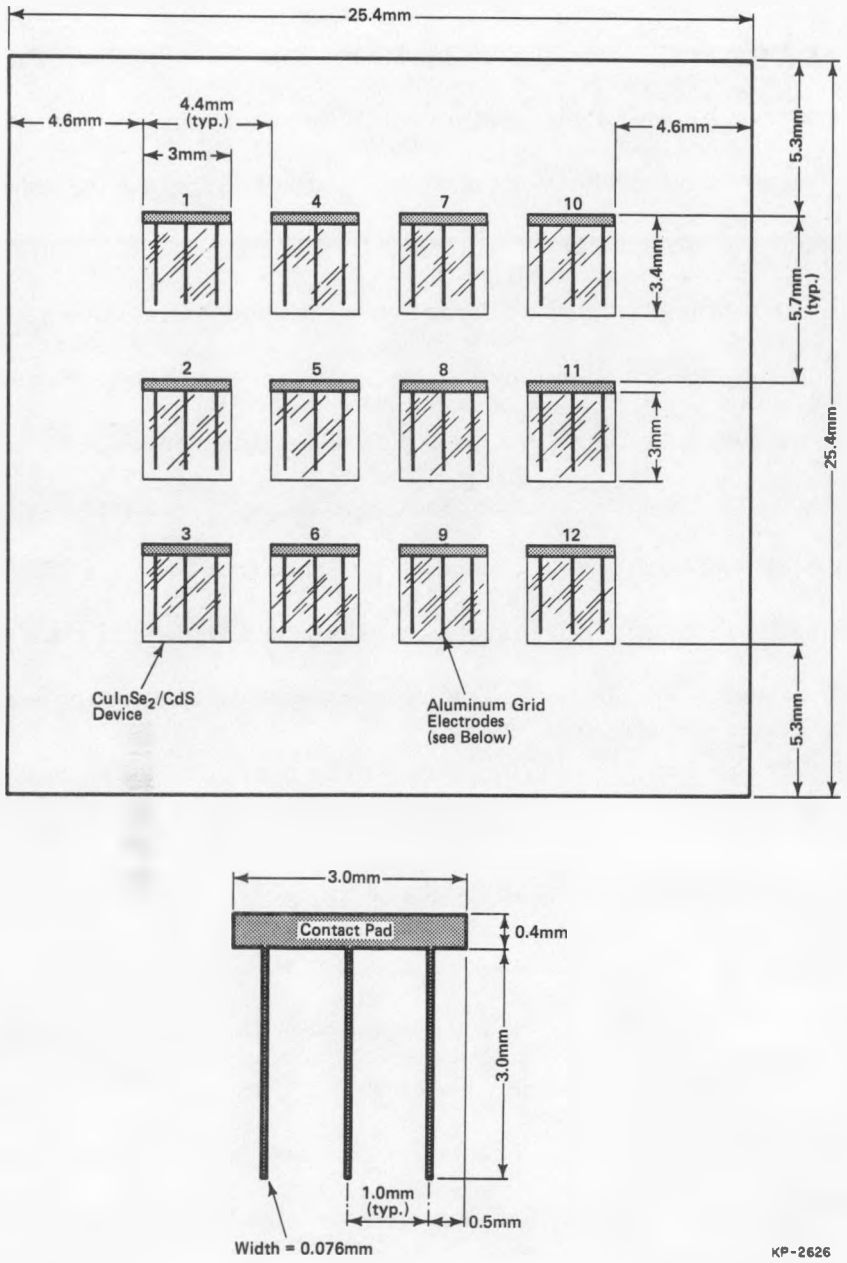

Fig. 20. Cell and grid configuration that will be used in initial phase of device fabrication activity at Illinois.

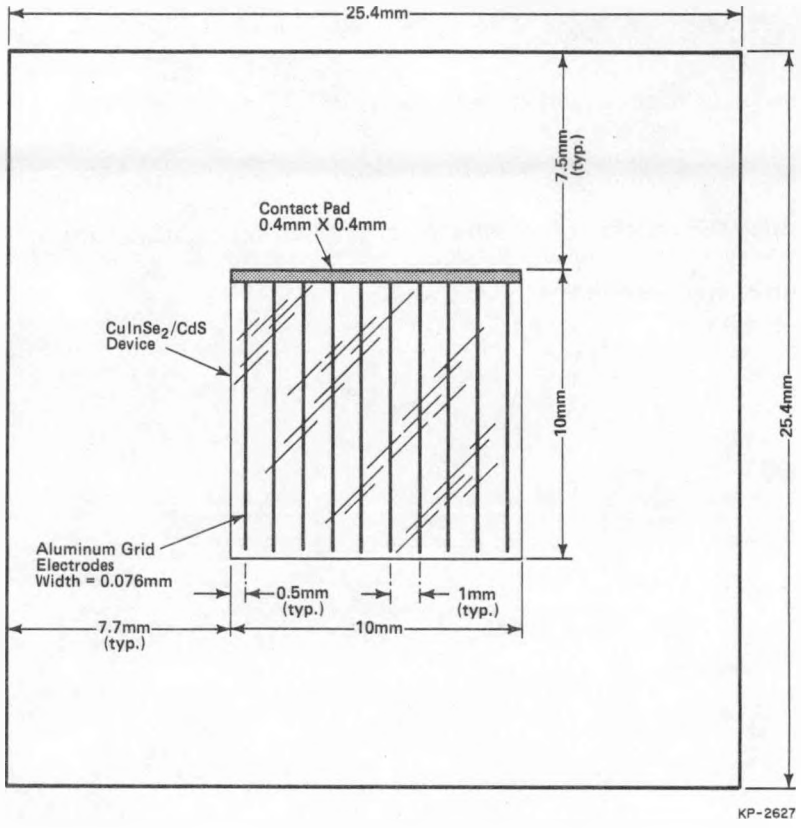

Fig. 21. Grid configuration that will be used for fabricating 1cm^2 cells.

will not be used at this stage of our work, since the primary objective is to compare $CuInSe_2$ layers and to demonstrate the general capabilities of the reactive sputtered $CuInSe_2$. Suitable photolithography equipment is available with the Coordinated Science Laboratory and at the adjacent Materials Research Laboratory. Photolithography masks have been prepared. It is anticipated that the cell fabrication activities will begin with the next few weeks.

Finally, an ultra-pure water system with provisions for substrate cleaning and rinsing has been installed. The system is shown schematically in Fig. 22. This installation is expected to significantly reduce the number of substrate-contamination-induced coating flaws which will assist in the fabrication of devices with thinner $CuInSe_2$ layers.

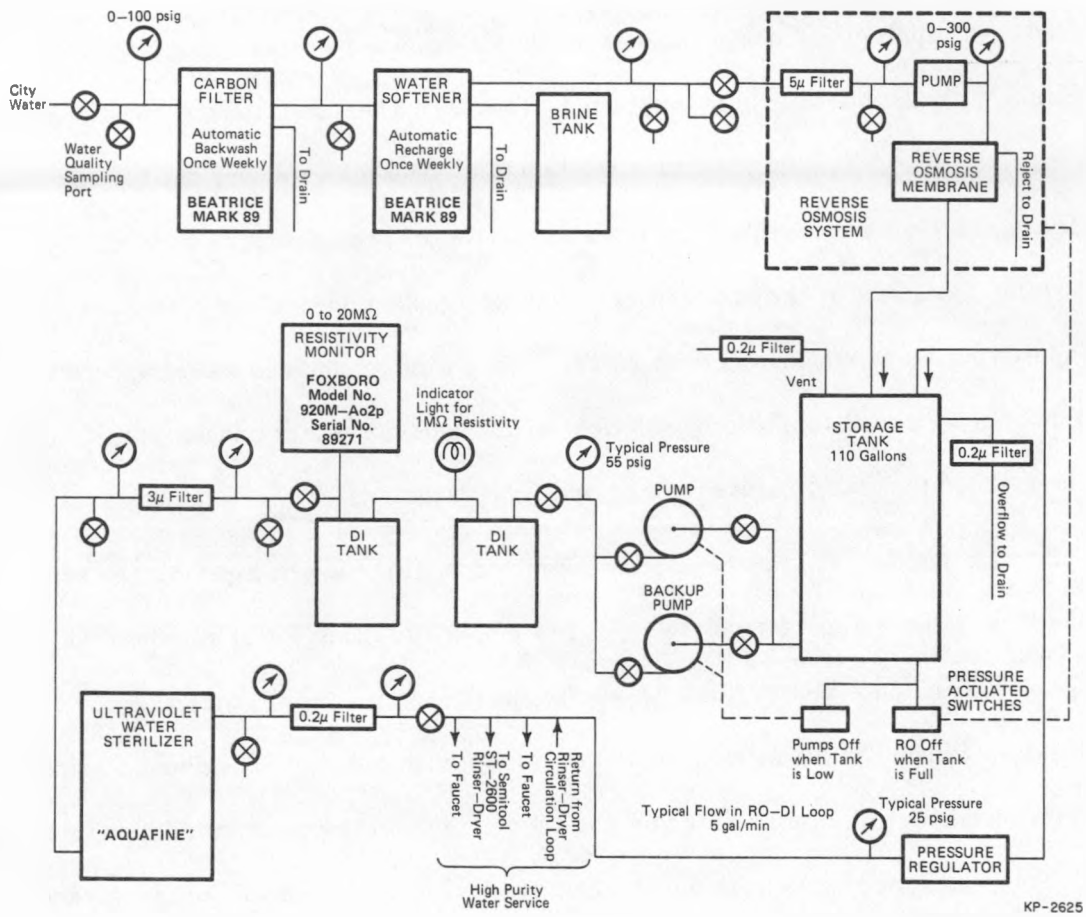

Fig. 22. Schematic illustration of ultra-pure water system.

6. SUMMARY STATUS

An in-line sputtering apparatus with a vacuum load lock and four deposition chambers, which permits all-sputtered $CuInSe_2/CdS$ heterojunctions to be fabricated without breaking vacuum, has been successfully moved from Telic Corporation to the University of Illinois and installed, with appropriate safety features, at the Coordinated Science Laboratory. Shakedown test for $CuInSe_2$ deposition have been completed (Task 2). The substrate transport system has now been used for over 500 runs without a malfunction. The placement of the Cu and In sputtering sources in the $CuInSe_2$ co-deposition chamber of the in-line apparatus significantly reduced the composition variations at the substrate that had been encountered in the preliminary $CuInSe_2$ reactive sputtering work which was done at Telic using a more confined radial apparatus. However, the gradients were still found to be sufficient to effect device performance. Therefore shields have now been added to further reduce these composition variations.

Characterization facilities have been assembled at Illinois which permit the following measurements: (1) device current-voltage and cell efficiency, (2) spectral response, (3) capacitance-voltage and capacitance-temperature, (4) surface photovoltage, and (5) optical absorption coefficient and bandgap (Task 1). An ultra-pure water system with substrate cleaning and rinsing facilities has been installed to assist in reducing the number of substrate-contamination induced coating flaws. This was done in anticipation of fabricating devices with thinner $CuInSe_2$ layers (Task 7).

Studies of the Cu-In-H_2Se reactive sputtering process have revealed two factors which introduce nonlinearities into the relationship between the deposition conditions and the properties of resultant coatings. The first is the formation of surface layers of modified composition on the target surfaces. The second is the fact that the elevated substrate temperatures that are used (typically 300-450°C) the In and Se sticking coefficients on the surface of the growing film are less than unity and dependent on the surface composition. Consequently the composition of the Cu-In-Se coatings is not proportional to the arriving coating flux. This latter consideration applies to evaporated as well as sputtered coatings and must be taken into account in selecting deposition condi-

tions. Despite this complexity we have demonstrated that coatings having compositions that are constant within about 2% can be consistently deposited by the reactive sputtering process once the sputtering targets have been conditioned.

A sub-contract is in place with the University of Delaware Institute of Energy Conversion whereby the Institute assists the Illinois group in material characterization and device fabrication. Our device fabrication work has followed the lead of the groups using vacuum evaporation for the $CuInSe_2$ deposition. Thus, in most cases we have used two-layer composite $CuInSe_2$ coatings which combine a high-resistivity In-rich top layer with a low resistivity Cu-rich base layer. The two layers appear to undergo an almost complete intermixing during deposition. Therefore we have experimented with base-layer and top-layer compositions that are considerably different than those used by most groups, but with thickness selected to give the same compositions in the composite coating. In particular, we have used base layers that were considerably richer in Cu (Cu = 32 at %, In = 21 at %, Se = 47 at %) than that used by most groups (Cu = 25.5 at %, In = 24.5 at %, Se = 50 at %). Nevertheless we have demonstrated that cells with reasonable efficiencies ($\eta \sim 5.5\%$) can be fabricated from this material provided that the composition of the resulting composite coating is in the same range which has yielded high performance cells from evaporated coatings.

The surface topography of the Cu-In-Se coatings is dependent on both the composition and the substrates temperature. The Cu-rich coatings which were used for the base layers in depositing the composite $CuInSe_2$ layers described above have an undersirably rough surface topography. This influences the structure of the overall composite layer and is believed to have been the cause of an electrical shorting problem which was encountered in many of the devices. Therefore in our future work we will reduce the Cu-composition and use base-layer/top-layer compositions that are very similar to those used by the groups using vacuum evaporation. Recent work has shown that very significant reductions in the roughness of the surface topography of the Cu-In-Se coatings can be obtained with modest adjustments in substrate temperature and coating composition.

The emphasis during the next two quarters will be on cell fabrication using the $CuInSe_2$ layers with the smoother surface topographies described above. Particular attention will be given to reducing the thickness of $CuInSe_2$ layer below the 3000 to 5000 nm range that is typically used. Cell fabrication will be done both at IEC and at Illinois. An important goal during this period will be to complete the development of cell fabrication capabilities at Illinois.

References

1) J.A. Thornton, D.G. Cornog, and J.D. Meakin, "Heterojunction Cell Research by Sputter Deposition," Final Report, Dec. 1, 1981 - January 31, 1983, SERI Contract XW-2-01313-1, Telic Publication No. 83-1, Telic Company, Santa Monica, CA (April 1983).

2) J.A. Thornton and D.G. Cornog, "$CuInSe_2$ Solar Cell Research by Sputter Deposition," Semiannual Technical Progress Report, Feb. 1, 1983 - Sept. 1, 1984, SERI Contract XL-2-02176-01, Telic Company, Santa Monica, CA, SERI Publication SERI/STR-211-2203 (September 15, 1983).

3) J.A. Thornton, D.G. Cornog, R.B. Hall, S.P. Shea and J.D. Meakin, "Preparation of $CuInSe_2$ Films by Reactive Co-Sputtering," in Proceedings of the Symposium on Materials and New Processing Technologies for Photovoltaics, ed. by J.A. Amick, V.K. Kapur, and J. Dietl, Vol. 83-11, The Electrochemical Society, Pennington, NJ (1983) p. 419.

4) J.A. Thornton, D.G. Cornog, R.B. Hall, S.P. Shea and J.D. Meakin, "Reactive Sputtered Cooper Indium Diselenide Films for Photovoltaic Applications," J. Vac. Sci. Technol. A, *2*, 307 (1984).

5) J.A. Thornton, D.G. Cornog, R.B. Hall, S.P. Shea and J.D. Meakin, "An Investigation of Reactive Sputtering for Depositing Copper Indium Diselenide Films for Photovoltaic Applications," Proceedings, Seventeenth IEEE Photovoltaic Specialists Conf. - 1984, IEEE, New York (1984) p. 781.

6) J.A. Thornton and T.L. Lommasson, "Magnetron Reactive Sputtering of Copper-Indium-Selenide, to be published Solar Cells (1985).

7) J.A. Thornton, T.C. Lommasson, A.F. Burnett, and J.W. Park, "$CuInSe_2$ Solar Cell Research by Sputter Deposition," Semiannual Technical Progress Report, December 21, 1984-June 30, 1985, SERI Contract XL-5-04131-1, University of Illinois at Urbana-Champaign (July 31, 1985).

8) C.A. Megerle, R.K. Gupta, G.A. Pollock, S.A. Vasquez, W.A. Chesarek, M.B.A. Monroe and V.K. Kapur, "Chemical and Optical Characterization of $CuInSe_2$ Thin Films for Solar Cells," in Proceedings of the Symposium on Materials and New Processing Technologies for Photovoltaics, ed. by J.A. Amick, V.K. Kapur, and J. Dietl, Vol. 83-11, The Electrochemical Society, Pennington, NJ (1983) p. 432.

9) R. Noufi, R. Axton, C. Herrington and S.K. Deb, "Electronic Properties Versus Composition of Thin films of $CuInSe_2$," Appl. Phys. Lett. *45*, 668 (1984).

10) L. Stolt, J. Hedström, M. Jargelius and D. Sigurd, "$CuInSe_2$ for Thin Films Solar Cells," paper presented at Sixth European Community Photovoltaic Conference, London, April 1985.

11) L. Stolt, M. Jargelius, J. Hedström, D. Sigurd and E. Niemi, "Growth of $CuInSe_2$ Thin Films," paper presented at Eighteenth IEEE Photovoltaic Specialists Conference, Las Vegas, NV, October 1985.

12) R.A. Mickelsen and W.S. Chen, "Polycrystalline Thin Film $CuInSe_2$ Solar Cells," in Proceedings Sixteenth IEEE Photovoltaic Specialist Conf., San Diego, CA (1982) p. 781.

13) R.A. Mickelsen and W.S. Chen, "Cadmium Sulfide/Copper Ternary Heterojunction Cell Research," Qtr. Techn. Prog. Rept., February 26, 1982-May 25, 1982, SERI Contract XJ-9-8021-1, Boeing Aerospace Company (July 1982).

14) T.W.F. Russell, R.E. Rocheleau, S.C. Jackson, and B.N. Baron, "Large Area Deposition of Semiconductor Thin Films: Chemical Reaction Engineering Fundamentals," paper presented at SERI Large Area Thin Film Photovoltaic Deposition Workshop, Golden, CO, June 24-25, 1985.

15) M.B. Robin, *Higher Excited States in Polyatomic Molecules*, vol. 1, Academic Press, New York, p. 276.

16) E. Stenhagen, S. Abrahamsson, and F.W. McLafferlyed, *Atlas of Mass Spectral Data*, Vol. 1, Interscience, New York (1969) p.7.

17) D.C. Dobson, F.C. James, I. Safarik, H.E. Gunning, and O.P. Strausz, "Photolysis of Hydrogen Selenide," J. Phys. Chem. *79*, 771 (1975).

18) L.S. Palatnik and E.I. Rogacheva, "Phase Diagrams and Structures of Some Semiconductor $A_2^I C^{VI} - B_2^{III} C^{VI}$ Alloys," Soviet Physics-Doklady, *12*, 503 (1967).

19) N.A. Goryunova, "*The Chemistry of Diamond-Like Semiconductors*," ed. by J.C. Anderson, MIT Press, Cambridge (1965).

20) T.L. Chu, S.S. Chu, S.S. Lin and J. Yue, "Large Grain Copper Indium Diselenide Films," J. Electrochem. Soc. *131*, 2183 (1984).

21) G. Masse and E. Radjai, "Radiative Recombination and shallow Centers in $CuInSe_2$," J. Appl. Phys., *4*, 1154 (1984).

22) J.A. Thornton and D.G. Cornog, "Cadmium Sulfide/Copper Sulfide Heterojunction Cell Research, final Rept. SERI Contract XJ-9-8033-2, Telic Publication No. 80-2, Telic Corporation, Santa Monica, CA (June 1980).

23) J.E. Jaffe and A. Zunger, "Electronic Structure of the Ternary Chalcopyrite Semiconductors $CuAlS_2$, $CuGaS_2$, $CuAlSe_2$, $CuGaSe_2$, and $CuInSe_2$," Physical Review B, *28*, 5822 (1983).

24) R. Noufi and J. Dick, "Compositional and Electrical Analysis of the Multilayers of a CdS/$CuInSe_2$ Solar Cell," J. Appl. Phys. *58*, 3884 (1985).